

OPTIMAL BOUNDED CONTROL AND RELEVANT
RESPONSE ANALYSIS FOR RANDOM VIBRATIONS

by

Daniil V. Iourtchenko

A Dissertation

Submitted to the Faculty

of the

WORCESTER POLYTECHNIC INSTITUTE

in partial fulfillment of the requirements for the

Degree of Doctor of Philosophy

in

Mechanical Engineering

by

_____(signature)_____

May 2001

APPROVED:

Professor Mikhail F. Dimentberg, Major Advisor
Mechanical Engineering Department

Professor Raymond R. Hagglund, Committee Member
Mechanical Engineering Department

Professor Zhikun Hou, Committee Member
Mechanical Engineering Department

Professor Suzanne L. Weekes, Committee Member
Department of Mathematical Sciences

Professor John M. Sullivan, Graduate Committee Representative
Mechanical Engineering Department

Abstract

In this dissertation, certain problems of stochastic optimal control and relevant analysis of random vibrations are considered. Dynamic Programming approach is used to find an optimal control law for a linear single-degree-of-freedom system subjected to Gaussian white-noise excitation. To minimize a system's mean response energy, a bounded in magnitude control force is applied. This approach reduces the problem of finding the optimal control law to a problem of finding a solution to the Hamilton-Jacobi-Bellman (HJB) partial differential equation. A solution to this partial differential equation (PDE) is obtained by developed 'hybrid' solution method. The application of bounded in magnitude control law will always introduce a certain type of nonlinearity into the system's stochastic equation of motion. These systems may be analyzed by the Energy Balance method, which introduced and developed in this dissertation. Comparison of analytical results obtained by the Energy Balance method and by stochastic averaging method with numerical results is provided. The comparison of results indicates that the Energy Balance method is more accurate than the well-known stochastic averaging method.

Acknowledgement

I would like to express my sincere appreciation to my advisor, professor Mikhail F. Dimentberg. His wise guidance and patience made this dissertation possible. I would like to thank him deeply for everything he has done for me, bringing me to WPI, giving me financial support for three years, and later bringing me to conferences and introducing me to members of scientific community.

I would like to thank my wife Tatiana Andreeva for being patient and supportive during all these years. Your constant love and support are helping me a lot.

I would like also to thank professors Z. Hou, J. Rencis, R. Hagglund, J Sullivan and their Russian colleagues A. Bratus' and V. Entov, for being very helpful, compassionate and always open for discussion. It was a great pleasure for me to associate with them for the last five years.

My thanks to the Mechanical Engineering Department, for giving me a chance to study here and for providing me a Teaching Assistantship. My special thanks to Barbara Edilberti, Barbara Furhman, Pamela St. Louis and Janice Dresser for all their help.

Table of Contents

Abstract	ii
Acknowledgement.....	iii
Table of Contents	iv
List of Figures	vii
List of Tables.....	viii
Nomenclature	ix
1. Introduction	1
2. Optimal Control.....	4
2.1 Stochastic Optimal Control	4
2.1.1 Introduction	4
2.1.2 The Hamilton –Jacobi-Bellman equation.....	5
2.1.3 Known solutions to the Hamilton-Jacobi-Bellman equation	9
2.2 Single-Degree-of-Freedom System with terminal cost function	12
2.2.1 Problem Statement	12
2.2.2 Analytical solution to the HJB equation for an “outer” domain	14
2.3 Single-Degree-of-Freedom System with integral cost function.....	16
2.3.1 Problem Statement	16
2.3.2 Analytical Solution to the HJB Equation for an “outer” domain.....	18
2.3.3 Analytical Solution to the HJB Equation for Boltz cost function.....	19
2.4 Numerical simulation of the HJB equation for an “inner” domain.....	21
2.4.1 Numerical Method.....	21
2.4.2 Results of numerical simulation for terminal cost function	24

2.4.3 Results of numerical simulation for integral and Boltz cost function..	31
2.5 Multi-Degree-of-Freedom System with terminal cost function.....	34
2.5.1 Problem statement	34
2.5.2 Analytical Solution to the HJB Equation for an “outer” domain.....	37
2.6 Multi-Degree-of-Freedom System with integral cost function	44
2.6.1 Problem statement	44
2.6.2 Analytical Solution to the HJB Equation for an “outer” domain.....	44
2.7 Dry friction is the optimal control law for steady-state response	46
2.8 Conclusions	47
3. Nonlinear random vibrations of Piecewise Conservative systems.....	49
3.1 Piecewise Conservative systems	49
3.2 Energy Balance Method.....	51
3.3 Piecewise Conservative systems - vibroimpact system	54
3.3.1 Application of Energy Balance method	54
3.3.2 Subharmonic response.....	59
3.3.3 Vibration of secondary structure	62
3.4 Piecewise Conservative systems – inertia controlled system.....	66
3.5 Piecewise Conservative systems – stiffness controlled system	71
3.6 Piecewise Conservative systems – pendulum with variable length	72
3.7 The Energy Balance method for a SDOF system with dry friction	74
3.8 Reliability analysis of a SDOF system with dry friction	77
3.9 Conclusions	80
4. Main Findings	82

5. Recommendations and future work.....	84
References	86

List of Figures

Figure 1. Computational domain for numerical simulation of the HJB equation	22
Figure 2. Level lines of expected energy $H(x_1, x_2, \tau) = 1$ and $\mu = 1.414$	25
Figure 3. Switching lines in phase plane for $\mu = 1.414$ for different values of τ :	26
Figure 4. Level lines of expected energy $H(x_1, x_2, \tau) = 1$ and $\mu = 2.121$	27
Figure 5. Switching lines in phase plane for $\mu = 2.121$ and different values of τ :	28
Figure 6. Level lines of relative difference, $\delta = (H_{sub} - H)/H$ for $\mu = 1.5$,	30
Figure 7. Comparison of switching Lines for Mayer and Lagrange cost functions.	32
Figure 8. Comparison of switching lines for Mayer, Lagrange and Boltz cost functions.	33
Figure 9. Optimal transformed control forces on a plane u_1, u_2	41
Figure 10. Optimal transformed control forces for various stiffnesses ratios,	42
Figure 11. Absolute percent deviations of analytical result from numerical one.	58
Figure 12. Application of α_{eq} for problem of subharmonic response.	61
Figure 13. Application of α_{eq} for problem of vibration of secondary structure.	65
Figure 14. Comparison of analytical with α_{eq} and numerical results.	66
Figure 15. Comparison of results for inertia controlled system.	70
Figure 16. Comparison of results for stiffness controlled system.	71
Figure 17. Comparison of results for a pendulum with variable length (swings).	74

List of Tables

Table 1. Maximal relative difference in energies $\max_{x_1, x_2} [(H_{sub} - H)/H]$, 30

Table 2. Nondimensional expected response amplitudes $\langle A \rangle \Omega^2 / R$ vs. $\mu = R / \sqrt{D\Omega}$ 76

Nomenclature

Symbols	Definitions
A	Transformation matrix
B	White-noise intensity matrix
D	Spectral density matrix
\mathcal{D}	An outer domain
E	An operation of averaging
E	Mean response energy of a system
f	Some function
\mathcal{G}	An outer domain
H	Bellman function for the terminal cost function
H	Distance to the rigid barrier
I	Identity matrix
K	Stiffness matrix
M	Mass matrix
\mathcal{Q}	Computational domain
r	Restitution coefficient
R	Bounds of optimal control
S	Bellman function for the integral cost function
S_{boltz}	Bellman function for the Boltz problem
T	Mean cycle duration time

t_f	Final time instant for control problem
W	Energy of a Multi-degree-of-freedom system
X	Displacement of a system
\dot{x}	Velocity of a system
y	Displacement of a system
\dot{y}	Velocity of a system
α_{eq}	Equivalent system's damping
Γ	An outer domain
\mathfrak{J}	The Lagrange or integral cost function
φ	The Mayer or terminal cost function
μ	Nondimensional parameter
Ω	Matrix of natural frequencies
ζ	Gaussian white-noise of unit intensity
σ	Intensity of white-noise
Θ	Cycle duration time

1. Introduction

Problems of optimal control have been known for a long time. However, only very simple, deterministic problems have been solved analytically because of the absence of computers and as a result the theory of control was not very popular. In the late 1940s, control theory gained a new impulse from the aerospace industry. Development of rockets, and later the launch of the first satellite increased interest in exploring this area. Because of the military and space applications of this theory, it became a priority topic at that time. Random loads were introduced into this theory, which gave a beginning to stochastic theory of control. Although today the theory of control may be encountered in different areas of engineering and science, this dissertation will only discuss problems of control for dynamic structures.

The work described in this dissertation is related to finding an optimal control law for an oscillatory system with bounded in magnitude control force applied to the system with the goal of minimizing a system's response energy. These problems, even in the simplest arrangement, are extremely difficult to solve analytically or numerically. The problems arising in processes of finding an optimal control law will be discussed later. In this dissertation, a new 'Hybrid' solution method has been proposed and implemented for solution of this problem. An exact analytical solution to the Hamilton-Jacobi-Bellman (HJB) equation within an 'outer' domain is obtained. This solution later is used to evaluate boundary conditions for numerical simulation of the HJB equation within the remaining 'inner' domain. Finally, an optimal control law for the system's response energy reduction is generated. An extremely important result is derived here for the

steady state system's response. It turns out that for the steady-state system's response, a 'dry-friction' control law is found to be the optimal one for mean response energy reduction.

Successful implementation of the 'hybrid' solution method has inspired us to continue and expand our research work in this area. Solution to the case of linear multi-degree-of-freedom (MDOF) systems has been found. This new 'hybrid' solution method opens a new way of looking onto the problems of stochastic optimal control. More intensive and profound investigations in this area are needed, especially with application in earthquake, aerospace and mechanical engineering.

Another challenging problem that we considered is the prediction the behavior of the optimally controlled system, subjected to random excitation. It may be shown on the example of stiffness controlled system, that such a system is conservative everywhere except at an extreme position as well as at a position of equilibrium, where due to optimal or 'bang-bang' control, the system's energy is reduced. As a result, a new name for such systems has been introduced. The term 'piecewise conservative' system is used to describe such a system with instantaneous or stepwise energy losses, occurring at discrete time instants. Since the system's mean response energy is of interest here, a new Energy Balance method is developed and implemented. This method provides us with an exact analytical expression for mean response energy in terms of mean cycle duration time. This mean duration time may be found as a solution to the first passage problem, which is represented as a partial differential equation. Because the first passage problem is a very complicated problem itself, its solution has been found by a perturbational approach. In the first approximation, the resulting mean cycle duration is found to be equal to the

system's natural period. The results obtained via the direct energy balance method for different systems were compared to results obtained by the stochastic averaging method as well as to those obtained by direct numerical simulation. This comparison has shown that the proposed and implemented direct energy balance method provides better accuracy than stochastic averaging method, far beyond expected applicability range of the latter. The simple explanation is that whilst both analytical methods require the mean response cycle duration to be close to the natural period of corresponding conservative system, the direct energy balance method, unlike the stochastic averaging method, does not require variations of the response energy within a cycle to be small.

The derivation of the HJB equation, the 'hybrid' solution method and its implementation will be discussed in details in Section 2. The energy balance method with various examples will be presented in Section 3. Basic findings and results of this dissertation will be summarized in Section 4. Section 5 will conclude this manuscript with some recommended direction for future work outlined in it.

2. Optimal Control

2.1 Stochastic Optimal Control

2.1.1 Introduction

In the late 1950s, Bellman proposed the Dynamic Programming method for solution of stochastic optimal control problems. According to this method, a problem of stochastic optimal control may be transformed into the problem of finding a solution to a certain partial differential equation (PDE) or so called the Hamilton-Jacobi-Bellman (HJB) equation, written for the Bellman function. At first, this method was accepted very well, but soon it was understood that this approach is very complicated and a lot of mathematical difficulties will have to be overcome. Consequently, only a few problems have been solved using this approach up.

Unfortunately, there has not been enough attention been paid to the Dynamic Programming method in the recent years. The main reason for this is its mathematical complexity. First of all, the HJB equation is a non-stationary, multidimensional partial differential equation. Secondly, if an introduced control force is bounded in magnitude, the operation of minimization (maximization) has to be performed. This leads to the appearance of nonlinear terms in the HJB equation. Moreover, this HJB PDE has to be solved within the entire state-space domain, whereas the behavior of the Bellman function at infinity is unknown. As a result, boundary conditions for the HJB equation are unknown and a simple numerical simulation of the HJB equation cannot be implemented. However the Dynamic Programming method has one advantage: solution to the HJB

equation is valid for entire state-space domain, so that there is no need to recalculate the same problem for different initial conditions.

2.1.2 The Hamilton –Jacobi-Bellman equation

When we talk about a system subjected to some random load, we should realize that it may not be possible to optimize some criteria with certainty. This leads to the concept of “stochastic” optimal control, where some averaged characteristics of a system are optimized rather than the randomly changing variables itself.

In generally, statement of control problems consists of three parts. The first part is governing equations of motion of the given dynamic system. It is a system of stochastic ordinary differential equations, which may be linear or non-linear. The second part deals with a control force, which usually belongs to a certain mathematical set. In other words, a control force may be unbounded or bounded in magnitude; some other restriction may be applied as well. Finally, the third part deals with so-called cost functional. This is actually a function that is to be minimized (maximized) by control force, introduced into equation of motion. The goal of the stochastic optimal control is to find an optimal control law, which belongs to given set from part two and minimizes (maximizes) given cost functional for the response, which satisfies governing equation of motion.

In all problems of optimal control there is a cost functional which has to be minimized (maximized). It may be the response displacement, velocity, energy or some combination of the above. The cost function (or cost functional) for stochastic optimal control problems is usually written (Stengel, 1986) as the Boltz cost function

$$J_1 = E \left[\varphi(\mathbf{x}(t_f), t_f) \right] + E \left[\int_{t_0}^{t_f} \mathfrak{L}(\mathbf{x}(s), \mathbf{u}(s), s) ds \right] \quad (2.1)$$

which is different from the deterministic cost function by operation of averaging of the right hand side (RHS) and $t_0 \leq s \leq t_f$. Here $E[\bullet]$ - is expected value, t_f is a final time instant, $\mathbf{u}(t)$ – control function and $\mathbf{x}(t)$ – vector of state variables. The first term, with $\varphi(\mathbf{x}(t_f), t_f)$ represents the Mayer or terminal cost function, whereas the second one $\int_{t_0}^{t_f} \mathfrak{L}(\mathbf{x}(s), \mathbf{u}(s), s) ds$ represents the Lagrange or integral cost function. Functions φ, \mathfrak{L} are certain functions, which form is known in advance. The first is usually encountered in problems when the difference in current system's position and the desirable position or the system's energy has to take the minimum value at the final time instant. The Lagrange cost function is used when a certain system's characteristics are to be minimized over all given time period $t_0 \leq s \leq t_f$.

Consider the minimization of a value function (which is related to the cost function as shown below) during the reduced time interval $[t_1, t_f]$, where $t_0 \leq t_1 \leq t_f$. Having found an optimal control \mathbf{u}^* in this time interval, the minimized value of cost function could be expressed as

$$J = \min_u J_1 = \min_u \left\{ E \left[\varphi(\mathbf{x}(t_f), t_f) \right] + E \left[\int_{t_1}^{t_f} \mathfrak{L}(\mathbf{x}(t), \mathbf{u}^*(t), t) dt \right] \right\} \quad (2.2)$$

A governing stochastic differential equation (SDE) of motion for a dynamic system may be generally written in the following vector form

$$\begin{aligned}\dot{\mathbf{x}}(t) &= \mathbf{f}(\mathbf{x}(t), \mathbf{u}(t), t) + \mathbf{L}(t)\boldsymbol{\zeta}(t) \\ \mathbf{x}(0) &= \mathbf{x}_0\end{aligned}\tag{2.3}$$

where \mathbf{L} is a matrix of disturbances $\boldsymbol{\zeta}(t)$, which is a Gaussian white-noise with the following characteristics

$$\begin{aligned}\mathbb{E}[\boldsymbol{\zeta}(t)] &= 0 \\ \mathbb{E}[\boldsymbol{\zeta}(t)\boldsymbol{\zeta}(t+\tau)] &= \mathbf{D}(t)\delta(t-\tau)\end{aligned}\tag{2.4}$$

The total derivative of J with respect to time is

$$\left. \frac{dJ}{dt} \right|_{t=t_1} = -\mathbb{E}[\mathfrak{J}(\mathbf{x}(t_1), \mathbf{u}^*(t_1), t_1)]\tag{2.5}$$

As an alternative, this derivative can be expressed by a series expansion. Retaining second-degree terms, the incremental change in J can be written (with partial derivatives evaluated at time t_1 as

$$\begin{aligned}\left. \frac{dJ}{dt} \Delta t \right|_{t=t_1} &= \mathbb{E} \left\{ \frac{\partial J}{\partial t} \Delta t + \frac{\partial J}{\partial \mathbf{x}} \dot{\mathbf{x}} \Delta t + \frac{1}{2} \left[\dot{\mathbf{x}}^T \frac{\partial^2 J}{\partial \mathbf{x}^2} \dot{\mathbf{x}} \right] (\Delta t)^2 + \dots \right\} \approx \\ &\mathbb{E} \left\{ \frac{\partial J}{\partial t} \Delta t + \frac{\partial J}{\partial \mathbf{x}} (\mathbf{f} + \mathbf{L}\boldsymbol{\zeta}) \Delta t + \frac{1}{2} (\mathbf{f} + \mathbf{L}\boldsymbol{\zeta})^T \frac{\partial^2 J}{\partial \mathbf{x}^2} (\mathbf{f} + \mathbf{L}\boldsymbol{\zeta}) (\Delta t)^2 \right\}\end{aligned}\tag{2.6}$$

Dividing both sides of (2.6) by Δt and replacing the last term by its trace, the time derivative is

$$\begin{aligned} \left. \frac{dJ}{dt} \right|_{t=t_1} &= \frac{\partial J}{\partial t} + \frac{\partial J}{\partial \mathbf{x}} \mathbf{f} + \frac{1}{2} \text{Tr} \left\{ \mathbf{E} \left[(\mathbf{f} + \mathbf{L}\boldsymbol{\zeta}) \frac{\partial^2 J}{\partial \mathbf{x}^2} (\mathbf{f} + \mathbf{L}\boldsymbol{\zeta})^T \right] \Delta t \right\} = \\ &= \frac{\partial J}{\partial t} + \frac{\partial J}{\partial \mathbf{x}} \mathbf{f} + \frac{1}{2} \text{Tr} \left\{ \mathbf{E} \left[\frac{\partial^2 J}{\partial \mathbf{x}^2} (\mathbf{f} + \mathbf{L}\boldsymbol{\zeta}) (\mathbf{f} + \mathbf{L}\boldsymbol{\zeta})^T \right] \Delta t \right\} \end{aligned} \quad (2.7)$$

Because \mathbf{x} and $\boldsymbol{\zeta}(t)$ are uncorrelated and taking the limit as $\Delta t \rightarrow 0$, yields

$$\begin{aligned} \frac{dJ}{dt} &= \frac{\partial J}{\partial t} + \frac{\partial J}{\partial \mathbf{x}} \mathbf{f} + \frac{1}{2} \lim_{\Delta t \rightarrow 0} \text{Tr} \left\{ \frac{\partial^2 J}{\partial \mathbf{x}^2} \left[\mathbf{E}(\mathbf{f}\mathbf{f}^T) \Delta t + \mathbf{L} \mathbf{E}(\boldsymbol{\zeta}\boldsymbol{\zeta}^T) \mathbf{L}^T \Delta t \right] \right\} = \\ &= \frac{\partial J}{\partial t} + \frac{\partial J}{\partial \mathbf{x}} \mathbf{f} + \frac{1}{2} \text{Tr} \left\{ \frac{\partial^2 J}{\partial \mathbf{x}^2} \mathbf{L} \mathbf{D} \mathbf{L}^T \right\} \end{aligned} \quad (2.8)$$

Combine now (2.5) and (2.8), and letting $t_1 = t$

$$\frac{\partial J}{\partial t} = - \left[\frac{\partial J}{\partial \mathbf{x}} \mathbf{f}(\mathbf{x}(t), \mathbf{u}^*(t), t) + \mathfrak{I}(\mathbf{x}(t), \mathbf{u}^*(t), t) + \frac{1}{2} \text{Tr} \left\{ \frac{\partial^2 J}{\partial \mathbf{x}^2} \mathbf{L} \mathbf{D} \mathbf{L}^T \right\} \right] \quad (2.9)$$

Because J is already the minimum of the cost function (2.2), it is independent of control law. Therefore, equation (2.9) does not have an implicit dependence on control law, although the optimal control \mathbf{u}^* may enter equation (2.9) explicitly.

Minimizing the time-rate-of-change of the value function by the choice of control

$$\frac{\partial J}{\partial t} = -\min_u \left[\frac{\partial J}{\partial \mathbf{x}} f(\mathbf{x}(t), \mathbf{u}^*(t), t) + \mathfrak{L}(\mathbf{x}(t), \mathbf{u}^*(t), t) + \frac{1}{2} \text{Tr} \left\{ \frac{\partial^2 J}{\partial \mathbf{x}^2} \mathbf{L} \mathbf{D} \mathbf{L}^T \right\} \right] \quad (2.10)$$

Equation (2.10) is called the Hamilton-Jacobi-Bellman (HJB) equation for Bellman function J . It is to be solved with initial condition $J(\mathbf{x}(t_f), t_f) = \varphi(\mathbf{x}(t_f), t_f)$. The approach based on this equation for solution of problems of optimal control is called Dynamic Programming method.

There are certain theorems [2, 19, 20, 22, 30] talking about uniqueness of solution to the HJB equation in case when SDE of motion (2.3) is linear. Moreover, the HJB equation (2.9) is only a sufficient condition for local optimality and it is not a necessary condition. The Bellman function might fail to satisfy differentiability and continuity conditions required to solve the partial differential equation, yet still be optimal.

The HJB equation is extremely difficult to solve because of the reasons, described in Section 2.1. Later we will consider an example of the HJB equation, where all the above difficulties will be seen.

2.1.3 Known solutions to the Hamilton-Jacobi-Bellman equation

Despite the mathematical difficulties discussed in the foregoing sections, certain exact and approximate solutions to the HJB equation are known for certain simple problems. Some solutions to the HJB equation are possible to obtain for the cases of unlimited in magnitude control force. One of the cases when an exact analytical solution exists is a linear-quadratic problem. Because control force is unbounded in magnitude in this problem, finding minimum is possible by differentiating the HJB equation with

respect to control force u . Condition of first derivative to be equal to zero provides the optimal control law, whilst the second derivative should be positive at that value of optimal control, in order to have minimum. This approach was implemented by (Zhu et. al. 1998) for Hamiltonian system. Although such statement of control problem is not very realistic there are cases when it could be justified. On the other hand an unbounded in magnitude force may not be feasible (Boyd S.P. et. al. 1991) and very often some bounds on control force have to be introduced. These types of problems will be considered in this dissertation.

Consider a simple example problem to illustrate how to derive the HJB equation for certain problem with bounded in magnitude control force [9]. Let

$$\begin{aligned}\dot{x}_1 &= x_2 \\ \dot{x}_2 &= u + \sigma\zeta(t)\end{aligned}\tag{2.11}$$

where σ^2 is a white-noise intensity. This equation describes the motion of a particle under influence of white-noise excitation. A bounded in magnitude control force $|u| \leq R$ is applied to the system in order to minimize a system's mean energy at final time instant. Therefore, Bellman function J may be chosen as

$$J = \min_{|u| \leq R} E \left\{ \frac{1}{2} [x_1^2(t_f) + x_2^2(t_f)] \right\}\tag{2.12}$$

Then, according to (2.9) the following HJB equation may be derived

$$\frac{\partial J}{\partial t} + \min_u \left[x_2 \frac{\partial J}{\partial x_1} + u \frac{\partial J}{\partial x_2} + \frac{\sigma^2}{2} \frac{\partial^2 J}{\partial x_2^2} \right] = 0 \quad (2.13)$$

Before trying to solve this equation, operation of minimization should take place. The Bellman function in (2.12) is already a minimum of the function on the right hand side and therefore is independent of control force as well as x_1, x_2 which are free parameters. As a result, only the second term in square brackets contain u and therefore the optimal control law is found as

$$\begin{aligned} \min_{|u| \leq R} \left\{ u \frac{\partial J}{\partial x_2} \right\} &= -R \left| \frac{\partial J}{\partial x_2} \right| \\ u &= -R \operatorname{sgn} \left\{ \frac{\partial J}{\partial x_2} \right\} \end{aligned} \quad (2.14)$$

Substituting (2.14) into equation (2.13) yields

$$\frac{\partial J}{\partial t} + x_2 \frac{\partial J}{\partial x_1} - R \left| \frac{\partial J}{\partial x_2} \right| + \frac{\sigma^2}{2} \frac{\partial^2 J}{\partial x_2^2} = 0 \quad (2.15)$$

As it can be seen, equation (2.15) is a nonlinear multidimensional PDE. In order to obtain an optimal control law defined by (2.14), one has to solve the HJB equation (2.15) first.

As we could see, the problem of finding solution to the HJB equation becomes much more complicated when applied control force is bounded in magnitude. The corresponding HJB equation is nonlinear because of the operation of minimization in the

RHS of equation (2.9). There are a number of books written about the Dynamic Programming approach [3, 10, 19–21, 26, 30, 34]. Several analytical solutions to this type of control problems have been obtained by perturbation approach [3, 5-7].

In reference [3], the author found the special case of the multidimensional in space HJB equation, which may be reduced under certain conditions to the one-dimensional in space HJB equation. This approach may not be used in the problems considered in this dissertation, because the abovementioned conditions are not satisfied. Moreover, solutions to the HJB equation, presented in this dissertation, obtained by method of characteristics.

Lets try to implement Dynamic Programming approach to specific problems considered in this dissertation.

2.2 Single-Degree-of-Freedom System with terminal cost function

2.2.1 Problem Statement

Consider a mass-spring system with deterministic initial conditions, subjected to a random excitation. A control force $u(t)$ is applied to the system, so that its equation of motion in terms of a displacement $x(t)$ may be written as

$$\begin{aligned} \ddot{x} + \Omega^2 x &= u(t) + \sigma(t)\zeta(t), \quad 0 \leq t \leq t_f \\ x(0) &= x_0, \dot{x}(0) = v_0 \end{aligned} \tag{2.16}$$

where $\zeta(t)$ is a standard zero-mean Gaussian white-noise of unit intensity, or derivative of a Wiener process and $\sigma^2(t)$ white-noise intensity. The control force is assumed to be of a bounded magnitude, i.e.

$$|u(t)| \leq R \quad (2.17)$$

According to the theory outlined in the previous sections, consider minimization problem for the mean response energy of the system at the given time instant t_f .

Introduce the Bellman function

$$H = \min_{|u| \leq R} E \left\{ \frac{1}{2} (\Omega^2 x_1^2 + x_2^2) \right\}_{t=t_f} \quad (2.18)$$

and a set of new state-space variables

$$\dot{x}_1 = x_2, \quad \dot{x}_2 = -\Omega^2 x_1 + u(t) + \sigma(t)\zeta(t) \quad (2.19)$$

The function H should satisfy the following HJB equation

$$\frac{\partial H}{\partial t} + x_2 \frac{\partial H}{\partial x_1} - \Omega^2 x_1 \frac{\partial H}{\partial x_2} + \min_{|u| \leq R} \left\{ u \frac{\partial H}{\partial x_2} \right\} + \frac{\sigma^2(t)}{2} \frac{\partial^2 H}{\partial x_2^2} = 0 \quad (2.20)$$

with condition $H(x_1, x_2, t_f) = (1/2)(\Omega^2 x_1^2 + x_2^2)$ imposed on H at final instant $t = t_f$.

Solution for the minimum in the left hand side (LHS) of the equation (2.20) yields

$$\min_{|u| \leq R} \{u(\partial H / \partial x_2)\} = -R|\partial H / \partial x_2|, \text{ where}$$

$$u = -R \operatorname{sgn}(\partial H / \partial x_2); \quad \operatorname{sgn} z = +1 \text{ for } z > 0, \operatorname{sgn} z = -1 \text{ for } z < 0 \quad (2.21)$$

Then, by introducing backward time $\tau = t_f - t$, the problem (2.20) is reduced to the following degenerate quasilinear PDE of parabolic type

$$\frac{\partial H}{\partial \tau} = x_2 \frac{\partial H}{\partial x_1} - \Omega^2 x_1 \frac{\partial H}{\partial x_2} - R \left| \frac{\partial H}{\partial x_2} \right| + \frac{\sigma^2(\tau)}{2} \frac{\partial^2 H}{\partial x_2^2} \quad (2.22)$$

with initial condition $H(x_1, x_2, 0) = (1/2)(\Omega^2 x_1^2 + x_2^2)$. If the solution is obtained for the PDE (2.22), the optimal control law is defined by the relation (2.21) for the given system's state (x_1, x_2) at given instant $\tau = t_f - t$. As long as the problem (2.22) is solved, the optimal control law can be designed using relation (2.21).

2.2.2 Analytical solution to the HJB equation for an “outer” domain

STATEMENT 1. The function

$$\begin{aligned} \tilde{H}(x_1, x_2, \tau) = & \frac{1}{2} \left\{ \left[x_2 - \frac{R \operatorname{sgn}(x_2)}{\Omega} \sin \Omega \tau \right]^2 + \left[\Omega x_1 + \frac{R \operatorname{sgn}(x_2)}{\Omega} (1 - \cos \Omega \tau) \right]^2 \right\} \\ & + B(\tau)/2; B(\tau) = \int_0^\tau \sigma^2(\gamma) d\gamma, \end{aligned} \quad (2.23)$$

provides an exact solution to the Cauchy problem for the equation (2.22) within the domain \mathbf{D} defined by the following inequality

$$\mathbf{D} = \left\{ (x_1, x_2, \tau) : |x_2| > \frac{R}{\Omega}, \tau \geq 0 \right\} \quad (2.24)$$

Proof. Upon substituting expression (2.23) into equation (2.22) the latter is reduced to

$$\frac{R^2}{\Omega} \sin \Omega \tau = x_2 R \operatorname{sgn}(x_2) - R \left| x_2 - \frac{R \operatorname{sgn}(x_2)}{\Omega} \sin \Omega \tau \right| \quad (2.25)$$

This equality is satisfied identically within domain \mathbf{D} , as defined by the inequality (2.24) and thus (2.23) is solution to equation (2.22) indeed. Q.E.D.

COROLLARY 1. The control law

$$u = -R \operatorname{sgn}(x_2) \quad (2.26)$$

is optimal within the “outer” domain D defined by the inequality (2.24). The proof is straightforward: relevant partial derivative of H is substituted into expression (2.21) and inequality (2.24) is used for its reduction. For vanishingly small R this simple “dry friction” control law becomes optimal everywhere except for a vanishingly small strip where the opposite to the inequality (2.24) holds. This is a limiting case of weak control, which can be studied by asymptotic methods. The dry friction control law for terminal cost function is sometimes called a suboptimal one, as being “asymptotically optimal” for vanishingly small R (case of “weak control”).

COROLLARY 2. If $H^0(x_1, x_2, \tau)$ is the solution to the problem (2.22) for the case $\sigma(t) \equiv 0$, the following bounds do exist then within domain (2.24):

$$0 \leq H(x_1, x_2, \tau) - H^0(x_1, x_2, \tau) = (1/2)B(\tau)$$

This estimate follows directly from an analytical solution (2.23) and illustrates well-known fact, that random excitation tends to increase a mean value of functional compare to one for deterministic problem.

2.3 Single-Degree-of-Freedom System with integral cost function

2.3.1 Problem Statement

Consider problem similar to the one, described in the foregoing section (2.19), but with different cost function. More precisely, consider the integral cost function, with the

mean system's energy being the function to minimize. The Bellman function may be introduced as following

$$S(x_1, x_2, t) = \min_u E \left[\int_t^{t_f} \frac{1}{2} (\Omega^2 x_1^2 + x_2^2) dt' \right] \quad (2.27)$$

The corresponding HJB equation in this case, will look similar to equation (2.20) with a term, added into the equation due to (2.27)

$$\frac{\partial S}{\partial t} + x_2 \frac{\partial S}{\partial x_1} - \Omega^2 x_1 \frac{\partial S}{\partial x_2} + \min_{|u| \leq R} \left(u \frac{\partial S}{\partial x_2} \right) + \frac{\sigma^2(t)}{2} \frac{\partial^2 S}{\partial x_2^2} + \frac{1}{2} (\Omega^2 x_1^2 + x_2^2) = 0 \quad (2.28)$$

with condition at final time instant $S(x_1, x_2, t_f) = 0$. Introducing backward time $\tau = t_f - t$, and calculating the minimum with respect to u

$$u = -R \operatorname{sgn} \left(\frac{\partial S}{\partial x_2} \right) \quad (2.29)$$

yields the same control law as in (2.21) but for function S , so that the HJB equation is

$$\frac{\partial S}{\partial \tau} = x_2 \frac{\partial S}{\partial x_1} - \Omega^2 x_1 \frac{\partial S}{\partial x_2} - R \left| \frac{\partial S}{\partial x_2} \right| + \frac{\sigma^2(\tau)}{2} \frac{\partial^2 S}{\partial x_2^2} + \frac{1}{2} (\Omega^2 x_1^2 + x_2^2) \quad (2.30)$$

and has to be solved with the initial condition $S(x_1, x_2, 0) = 0$. Solution to the nonlinear PDE (2.30) provides the optimal control law (2.29).

2.3.2 Analytical Solution to the HJB Equation for an “outer” domain

Lets introduce the "outer" domain, defined as

$$\Gamma = \left\{ x_1, x_2, \tau : |x_2| > \left| \frac{R}{\Omega^2 \tau} (\cos(\Omega \tau) - 1) \right| \right\} \quad (2.31)$$

STATEMENT 2. The function

$$S(x_1, x_2, \tau) = \frac{1}{2} (\Omega^2 x_1^2 + x_2^2) \tau + \frac{R \operatorname{sgn} x_2}{\Omega^2} \left[\Omega^2 x_1 \tau + x_2 (\cos(\Omega \tau) - 1) - \Omega x_1 \sin(\Omega \tau) \right] + \frac{R^2}{\Omega^2} \left[\tau - \frac{\sin(\Omega \tau)}{\Omega} \right] + \Lambda(\tau), \quad (2.32)$$

$$\text{where } \Lambda(\tau) = \int_0^\tau \frac{\sigma^2(\chi)}{2} \chi d\chi$$

is the exact solution to equation (2.30) within Γ .

Proof. Substituting (2.32) into equation (2.30), results after some cancellations in

$$-\frac{R^2}{\Omega^2} (\cos(\Omega \tau) - 1) - R |x_2| \tau = -R \left| \frac{R \operatorname{sgn} x_2}{\Omega^2} (\cos(\Omega \tau) - 1) + x_2 \tau \right| \quad (2.33)$$

It can be seen by inspection that two sides of equation (2.33) are indeed equal if inequality (2.31) holds, thereby indicating that (2.32) is the solution to the HJB equation (2.30). The "inner" domain here represents a strip of a finite width in x_2 , infinite in $\pm x_1$ direction and symmetric with respect to $x_2 = 0$. It is worth mentioning that with increase of backward time τ to some certain value and beyond, inequality (2.31) will always hold. In this case the "inner" domain will be shrinking to a line $x_2 = 0$. The solutions within the "inner" domains for both abovementioned problems (2.31) will be obtained numerically in the next section.

2.3.3 Analytical Solution to the HJB Equation for Boltz cost function

Having obtained solutions for the Mayer (Bratus et. al., 2000) and Lagrange (Iourtchenko 2000) cost functions one can develop solution to the Boltz problem. A linear combination of these solutions will represent an analytical solution for the Boltz cost function, within the "outer" domain. Denote the Bellman function, corresponding to the Boltz problem as

$$S_{boltz} = \min_u \left\{ E \left[\frac{a_1}{2} (\Omega^2 x_1^2(t_f) + x_2^2(t_f)) \right] + E \left[\frac{a_2}{2} \int_t^{t_f} (\Omega^2 x_1^2 + x_2^2) dt' \right] \right\} \quad (2.34)$$

The HJB equation for this case is the same as (2.30), with the last term in the RHS multiplied by a_2 . The initial condition for the Boltz problem would be taken from the Mayer problem as $S_{boltz}(x_1, x_2, 0) = 1/2(\Omega^2 x_1^2 + x_2^2)$. Then, a linear combination of

solutions (2.23) and (2.32) is a solution to problem (2.34) within the following "outer" domain \mathbf{G} , defined as

$$\mathbf{G} = \left\{ x_1, x_2, \tau : |x_2(a_1 + a_2\tau)| > \left| \frac{R}{\Omega} \left(a_2 \frac{\cos(\Omega\tau) - 1}{\Omega} - a_1 \sin(\Omega\tau) \right) \right| \right\} \quad (2.35)$$

The optimal control law for the Boltz cost function is defined as $u = -R \operatorname{sgn}(\partial S_{\text{Boltz}} / \partial x_2)$. It is possible to coordinate the contribution of each solution into formula for final solution by using different values of these factors.

The solutions for the terminal, integral and Boltz cost functions are valid for arbitrary temporal variations of noise intensity $\sigma(t)$. Consequently, these results can be directly applied to the problems with time varying noise intensity, such as earthquake for instance. For the constant value of noise intensity, which is considered in this work, $\Lambda(\tau) = \sigma^2 \tau^2 / 4$ and $B(\tau) = \sigma^2 \tau / 2$.

Concluding this section the next, very important fact should be stressed here. Namely, since the exact explicit analytical solutions are found, the exact boundary conditions, rather than approximate ones (Bratus, 1975), are imposed for numerical simulations of the HJB equation. Therefore the optimal control laws obtained numerically by means of the "hybrid" method are high precision ones, valid for any, not small values of R and σ .

2.4 Numerical simulation of the HJB equation for an “inner” domain

2.4.1 Numerical Method

To find an optimal control law for all values of x_1, x_2, τ one must find solution to the equation (2.22) and (2.30) within the “inner” domain. The available analytical solutions are extremely helpful in handling a problem of infinite overall domain, since it can be used to obtain boundary conditions for numerical solution of these equations within a bounded expanded “inner” domain. Specifically, the following computational domain \mathbf{Q} was used for numerical solutions

$$|x_2| \leq d_2, |x_1| \leq d_1 \quad (2.36)$$

Here d_2 should be taken so that, inequality (2.24) or (2.31) holds for all values of backward time. As long as both the HJB PDEs are of a parabolic type in τ and x_2 , the boundary conditions (BCs) should be assigned on the top and bottom part of computational domain, that is, at $x_2 = \pm d_2$. This can be very simply implemented with the use of the analytical solutions.

On the other hand, both PDEs are hyperbolic in τ and x_1 , with characteristics of the hyperbolic part being $dx_1/d\tau = -x_2$, $x_2\tau - x_1 = \text{const}$. Therefore, x_1 decreases along characteristics if $x_2 > 0$ and increases if $x_2 < 0$. Thus, the BCs in x_1 should be assigned

along those parts of the boundary $|x_1| = d_1$ only, where the characteristics enter into \mathbf{Q} , that is, for

$$x_1 = d_1 \text{ if } x_2 > 0, \quad x_1 = -d_1 \text{ if } x_2 < 0 \quad (2.37)$$

This part of the boundary will be denoted by \mathbf{Q}_1 . It is illustrated by bold lines in Figure 1, where directions of characteristics are also shown (by arrows). At the remaining part of the boundary $|x_1| = d_1$ no BCs are needed.

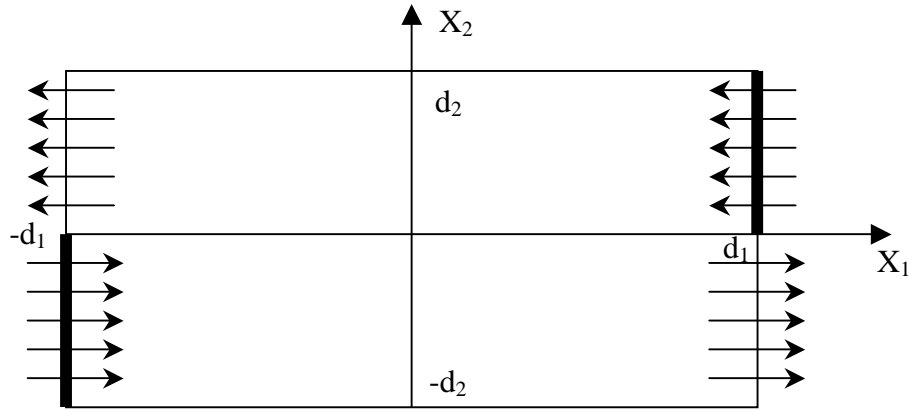


Figure 1. Computational domain for numerical simulation of the HJB equation

Numerical solution to both equations is based on the explicit and unconditionally stable DuFort-Frankel scheme (Anderson et al., 1984). The necessary values of the function H and its derivatives at the boundaries are easily obtained from the analytical solutions. Let, for instance $H_{i,j}^k$ be value of H at the point $x_1^i = ih_1, x_2^j = jh_2, \tau^k = k\Delta\tau$, where $h_1, h_2, \Delta\tau$ are steps in x_1, x_2, τ respectively. Then

$$\begin{aligned} (1/2\Delta\tau)(H_{i,j}^{k+1} - H_{i,j}^{k-1}) = & (jh_2/2h_1)(H_{i+1,j}^k - H_{i-1,j}^k) - (\Omega^2 ih_1/2h_2)(H_{i,j+1}^k - H_{i,j-1}^k) - \\ (R/2h_2)|H_{i,j+1}^k - H_{i,j-1}^k| + & (\sigma_k^2/2h_2^2)(H_{i,j+1}^k - H_{i,j}^{k-1} + H_{i,j-1}^k - H_{i,j}^{k+1}); \quad \sigma_k = \sigma(\tau^k) \end{aligned} \quad (2.38)$$

Equations (2.38), representing a discretization of (2.22), allow us to determine values of H at all nodal points in \mathbf{Q} except for those at \mathbf{Q}_1 . To find values of H at \mathbf{Q}_1 , we represent $\partial H/\partial x_1$ at \mathbf{Q}_1 in the form

$$\begin{aligned} \left. \frac{\partial H}{\partial x_1} \right|_{x_1=-d_1} &= \frac{-3H_{1,j}^k + 4H_{2,j}^k - H_{3,j}^k}{2h_1} + o(h_1^2) \\ \left. \frac{\partial H}{\partial x_1} \right|_{x_1=+d_1} &= \frac{3H_{m,j}^k - 4H_{m-1,j}^k + H_{m-2,j}^k}{2h_1} + o(h_1^2) \end{aligned} \quad (2.39)$$

Using formulae (2.39) in equations (2.38) for $i = 1$ and $i = m$, one can find solution along \mathbf{Q}_1 . Finite-difference scheme for the Lagrange and Boltz cost functions will be very similar to one, described above.

The calculations were performed for $\Omega = 1$. Consequently, it is easy to show that inequality (2.31) is bounded within $|x_2| \geq 1.5 R/\Omega$. Therefore, the computational domain of the following size $d_1 = d_2 = 4$, is considered. The following values of increments in the finite-difference scheme had been used: $h_1 = h_2 = 0.05; \Delta\tau = 0.001$, thereby satisfying the condition $\Delta\tau \ll h_j, j = 1, 2$, as suggested by Anderson et. al. (1984). The convergence of the numerical solution had also been verified by repeating calculations for selected cases with twofold reduction of both spatial steps.

For the case of a stationary white-noise excitation the important nondimensional parameter is used as $\mu = R/(\sigma\sqrt{\Omega}) = \Delta/(2\sigma_c)$; $\Delta = R/\Omega^2$, $\sigma_c = \sigma/(2\Omega^{3/2})$. Here Δ is clearly seen to be a static displacement due to a constant force with magnitude being equal to that of the maximum control force, whereas σ_c is a steady-state root mean square (RMS) displacement response to a white-noise of a SDOF system with *critical* value of linear viscous damping.

2.4.2 Results of numerical simulation for terminal cost function

Obviously the best way to represent the results is to compare the system` energy alternation in time for controlled and uncontrolled systems. However it is proved to be time-consuming procedure. Namely, to do this one should solve numerically the HJB equation on every time step, determine the sign of the optimal control law, return to the Monte Carlo simulation and proceed to the next time interval. Therefore, presentation of results will be in the form of Bellman function and its derivative.

Figure 2 illustrates level lines of expected energy $H(x_1, x_2, \tau) = 1$ for different values of the "backward" time $\tau = t_f - t$ and $\mu = \sqrt{2} = 1.414$. The values of H inside the enclosed curves, for the corresponding values of backward time, are less than unity and consequently more the unity outside these enclosed curves. The solution is clearly seen to be anti-symmetric within the lower half of the phase plane. Progressive "shrinking" of the enclosed areas is seen with decreasing "backward" time τ - therefore with real time t approaching the final time instant. This illustrates actual reduction of the original response energy to its final value $H = 1$ (which is used as a label for all these

curves). Figure 3 illustrates evolution of the corresponding switching lines on the phase plane, defined as the lines with $\partial H/\partial x_2 = 0$. They are used for choosing proper sign, or direction for the optimal control force, as long as the above partial derivative is positive above the relevant switching line and negative below it.

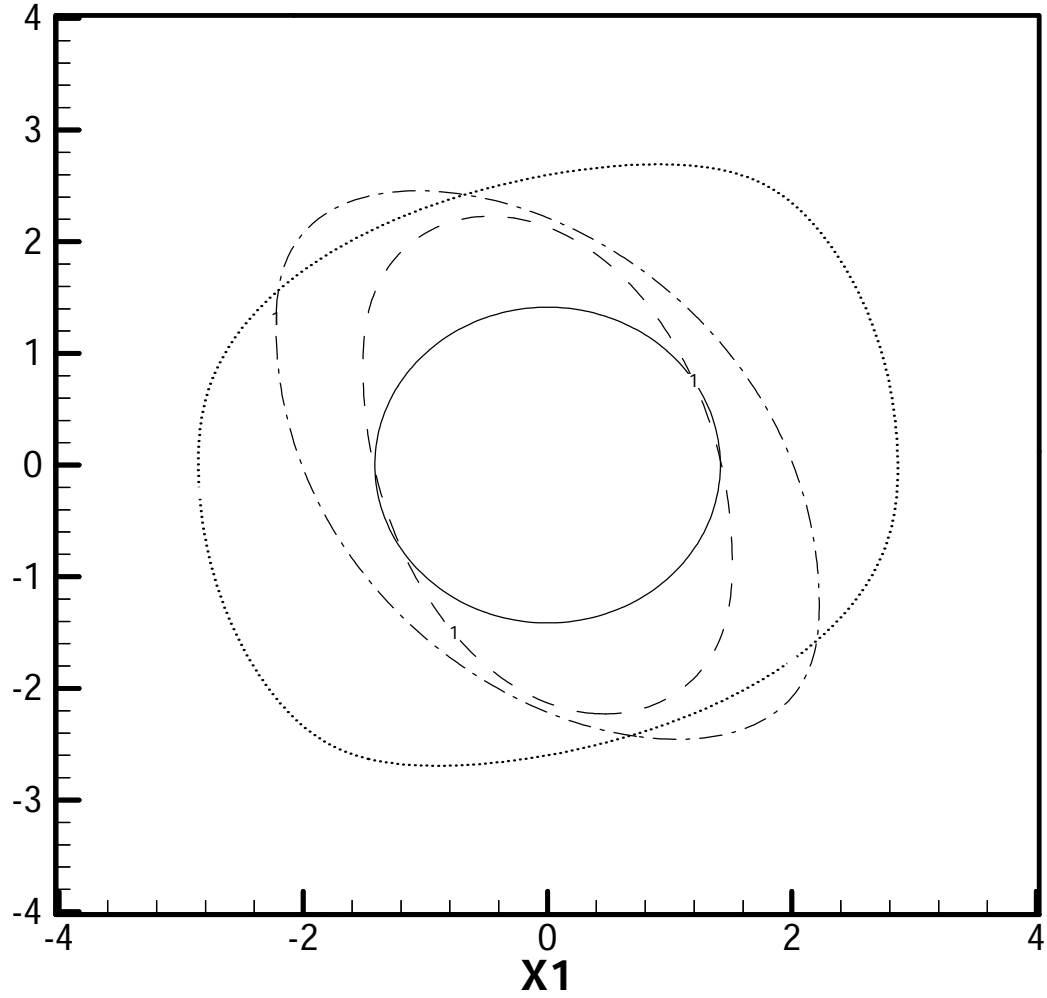


Figure 2. Level lines of expected energy $H(x_1, x_2, \tau) = 1$ and $\mu = 1.414$ for different values of τ : 0 for solid, $\pi/4$ for dashed, $\pi/2$ for dash-dot, π for dotted.

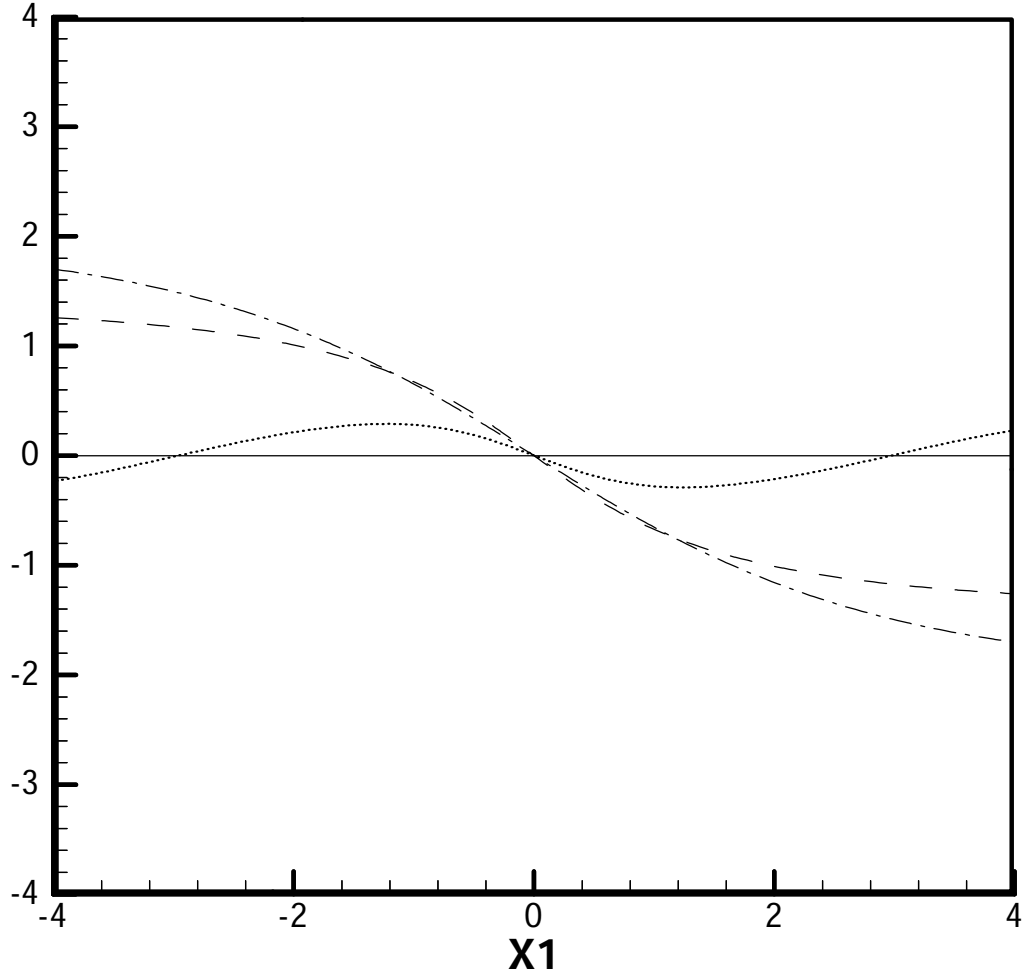


Figure 3. Switching lines in phase plane for $\mu = 1.414$ for different values of τ :

0 for solid, $\pi/4$ for dashed, $\pi/2$ for dash-dot, π for dotted.

Figure 4 illustrates similar level lines of the expected energy $H = 1$ for the case $\mu = 1.5 \cdot \sqrt{2} = 2.121$, which corresponds to higher R . It can be seen clearly, that larger reduction of the response energy is possible with the increased upper bound R on the available control force, that is, with increased control resources. Namely, value of energy at any given instant τ , which can be reduced to $H = 1$ by the time instant t_f , is found to be larger than one given in Figure 2 for the same τ but with the smaller R .

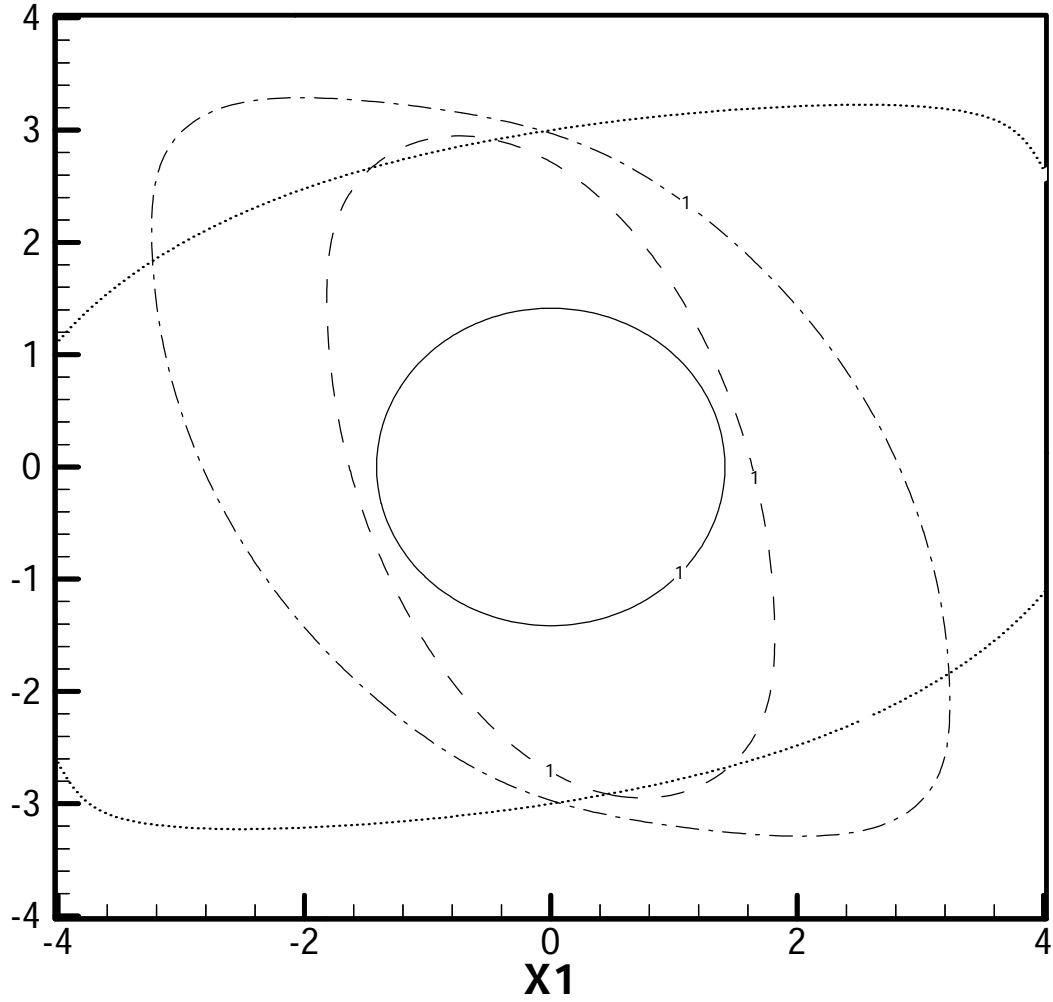


Figure 4. Level lines of expected energy $H(x_1, x_2, \tau) = 1$ and $\mu = 2.121$

for different values of τ : 0 for solid, $\pi/4$ for dashed, $\pi/2$ for dash-dot, π for dotted.

The corresponding switching lines, as shown in Figure 5, are seen to lie further from the abscissa than those in Figure 3 (for the same nonzero time instants). As long as this abscissa corresponds to the simple dry-friction control law, this means that increasing

bound on the available control force R makes the optimal control law less close to the asymptotically suboptimal one, which corresponds to the case of a weak control.

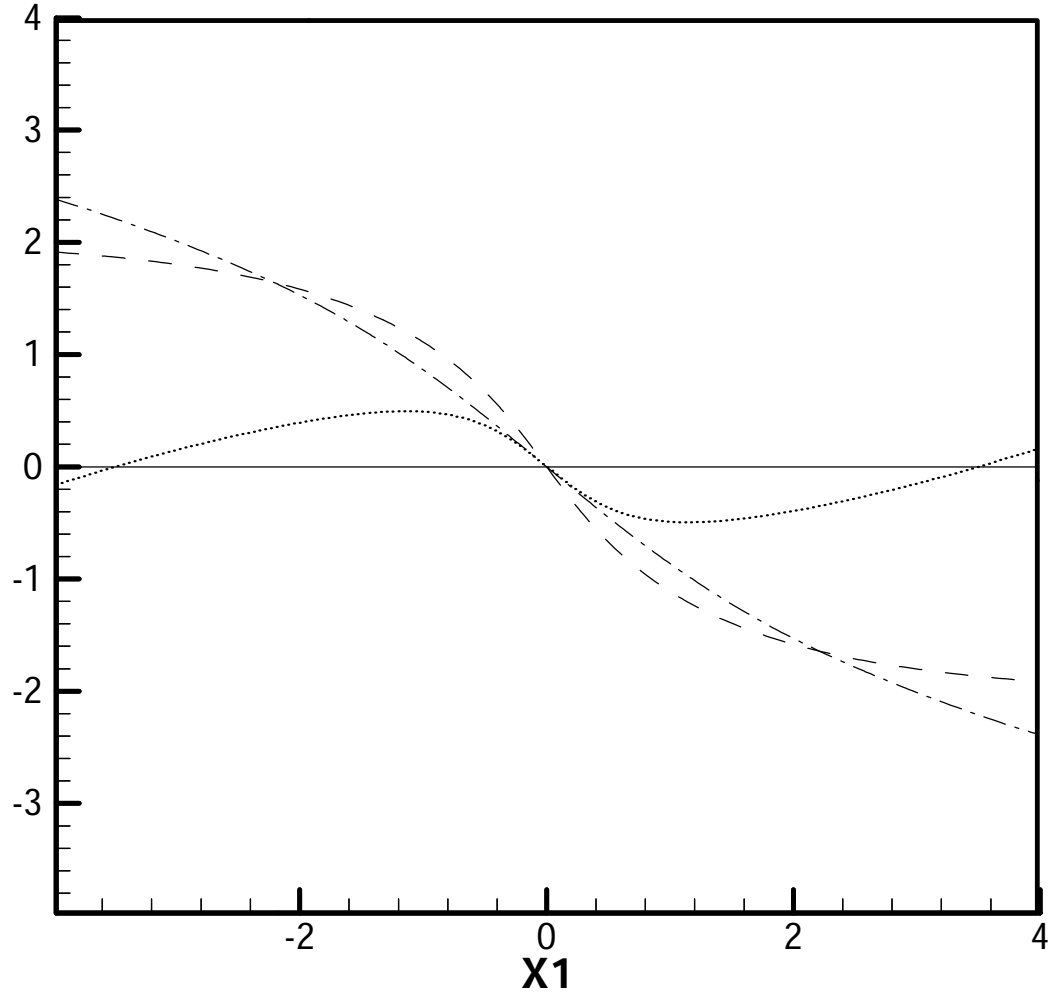


Figure 5. Switching lines in phase plane for $\mu = 2.121$ and different values of τ :
0 for solid, $\pi/4$ for dashed, $\pi/2$ for dash-dot, π for dotted.

Figure 6 and Table 1 contain further results of numerical evaluation of the dry-friction control law. In the asymptotic theory, where both R and σ^2 are assumed to be proportional to a small parameter, the difference in the values of the minimized (energy)

functional is known to be proportional to the same small parameter; it is precisely in this sense that the control law (2.21) may be regarded as a suboptimal one. The present solution provides a possibility for numerical evaluation of the "degree of suboptimality" for finite values of the supposedly small parameters. Namely, relative differences $\delta = (H_{sub} - H)/H$ were calculated for two different time instants. Here H is the result of the present "hybrid" solution for the strictly optimal control case, whereas subscript 'sub' refers to the case of the "suboptimal" control. These values of H for the suboptimal case were calculated by applying the basic procedure for calculating the hybrid solution to the appropriately modified HJB equation (2.22) – namely, with the term $-R|\partial H/\partial x_2|$ replaced by $-R(\partial H/\partial x_2)\text{sgn } x_2$. Figure 6 illustrates lines of constant level of δ in the phase plane for $\tau = \pi, \mu = 1.5$. Two (anti-symmetric) peaks can be seen here, with a valley containing saddle-points between them. The peak value was found to be 0.7376. The same double-peak pattern has been observed for other values of μ .

The results of evaluation of the suboptimal dry-friction control law vs. the optimal one are summarized in the Table 1. Here maximal values of δ within the phase plane are presented for different values of R and two different time instants. As should be expected, the deviation from perfect optimality increases monotonously with R , or μ , within the range considered. The case $\mu \ll 1$ may be regarded as a suboptimal one indeed, and even at $\mu = 1$ the maximal difference in H is seen to be about 15 per cent

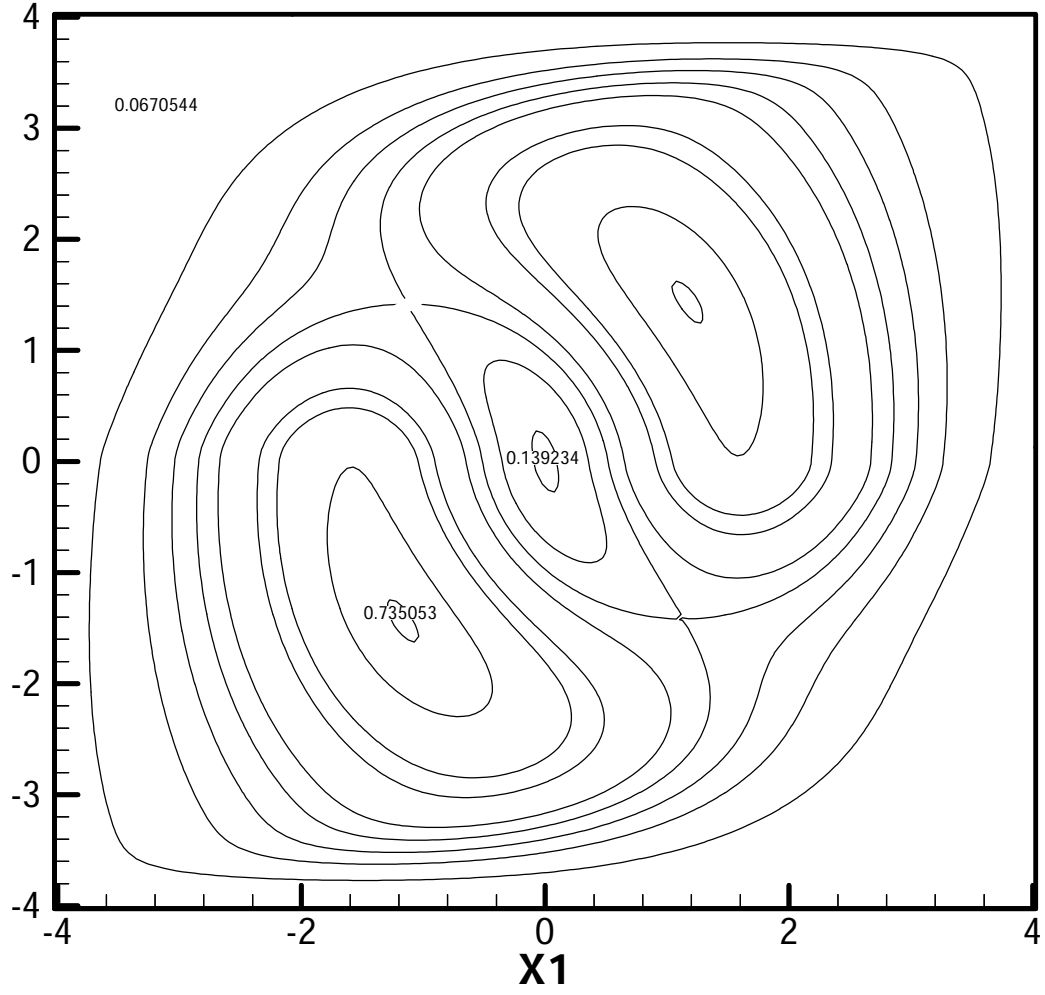


Figure 6. Level lines of relative difference, $\delta = (H_{sub} - H)/H$ for $\mu = 1.5$, obtained for the cases of optimal and 'suboptimal' (dry-friction) control laws

	μ	0.5	0.8	1	1.5	2	2.5
τ							
$\pi/2$		$1.7 \cdot 10^{-2}$	$7.54 \cdot 10^{-2}$	0.155	0.606	1.718	4.16
π		$1.25 \cdot 10^{-2}$	$6.26 \cdot 10^{-2}$	0.142	0.757	2.949	10.33

Table 1. Maximal relative difference in energies $\max_{x_1, x_2} [(H_{sub} - H)/H]$, as obtained for the cases of optimal and "suboptimal" (dry-friction) control

only. On the other hand, larger increases in H with deviations from the perfectly optimal control can be seen at $\mu = 1.5$, and especially at values higher than two.

2.4.3 Results of numerical simulation for integral and Boltz cost function

Figure 7 demonstrates the switching lines $\partial S / \partial x_2 = 0$ for the terminal and integral types of cost functions evaluated for $\mu = \sqrt{2}$ at two different instants of backward time. This plot clearly shows how different two optimal control laws may be. In particular, optimal switching lines for integral control are seen to be much less sensitive to the final control time than those for the terminal control.

Because the switching line $\partial S / \partial x_2 = 0$ plays crucial role in defining the optimal control law another set of switching lines is to be presented. Figure 8 demonstrates the switching lines obtained for the Mayer, Lagrange and Boltz cost functions for $\mu=2.121$. It seems that switching lines for the Lagrange and Boltz type cost functions are not very much different compared to one corresponding to the Mayer cost function. This type of behavior was observed during the all backwards time. As a result, in a sense of optimal control law, the Boltz problem can be better "approximated" by the Lagrange problem, for the specific types of cost functions, taken in this paper. Nevertheless, it is clear that all of these problems provide different, unique optimal control law.

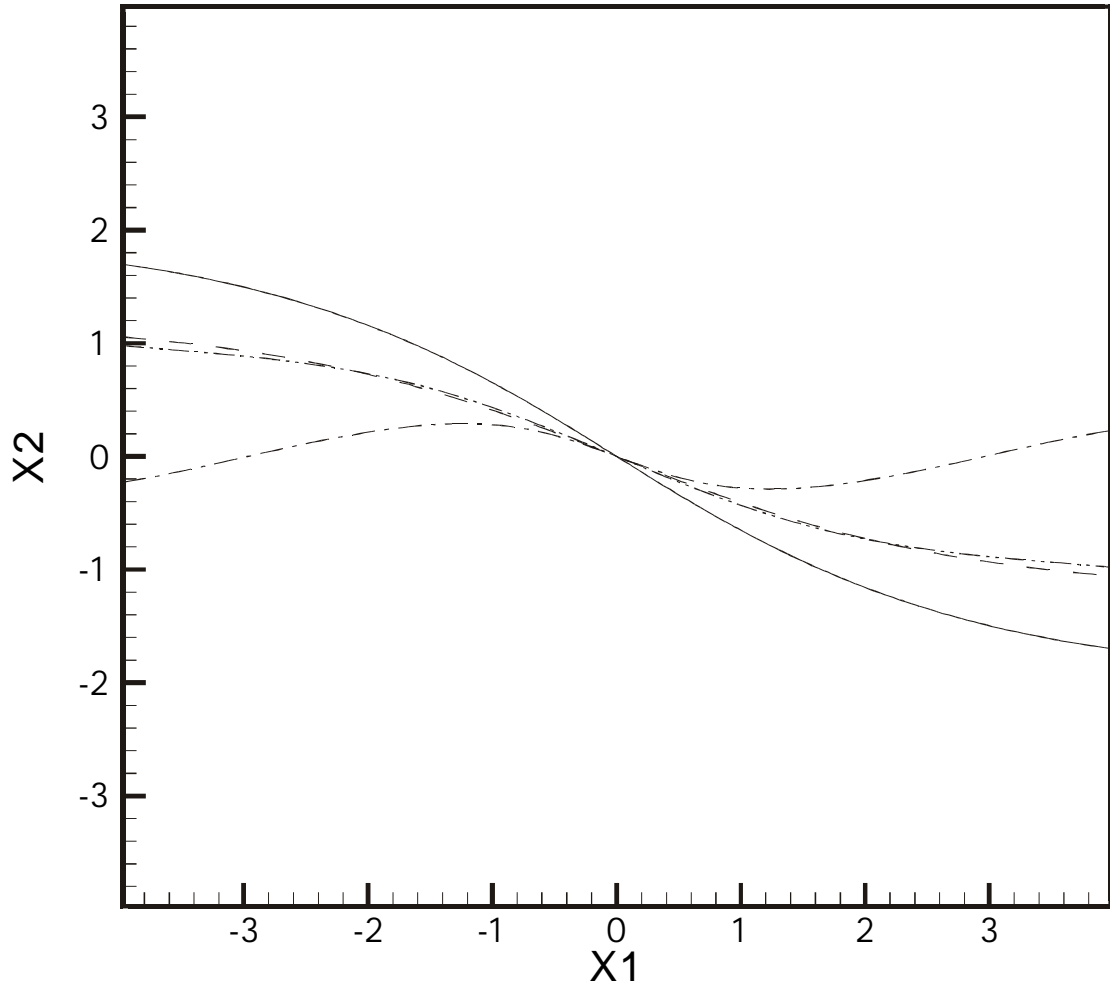


Figure 7. Comparison of switching Lines for Mayer and Lagrange cost functions.

Solid – the Mayer cost function, dashed – the Lagrange cost function for $\tau = \pi/2$. dash-dot – the Mayer cost function, dash-dot-dot – the Lagrange cost function for $\tau = \pi$.

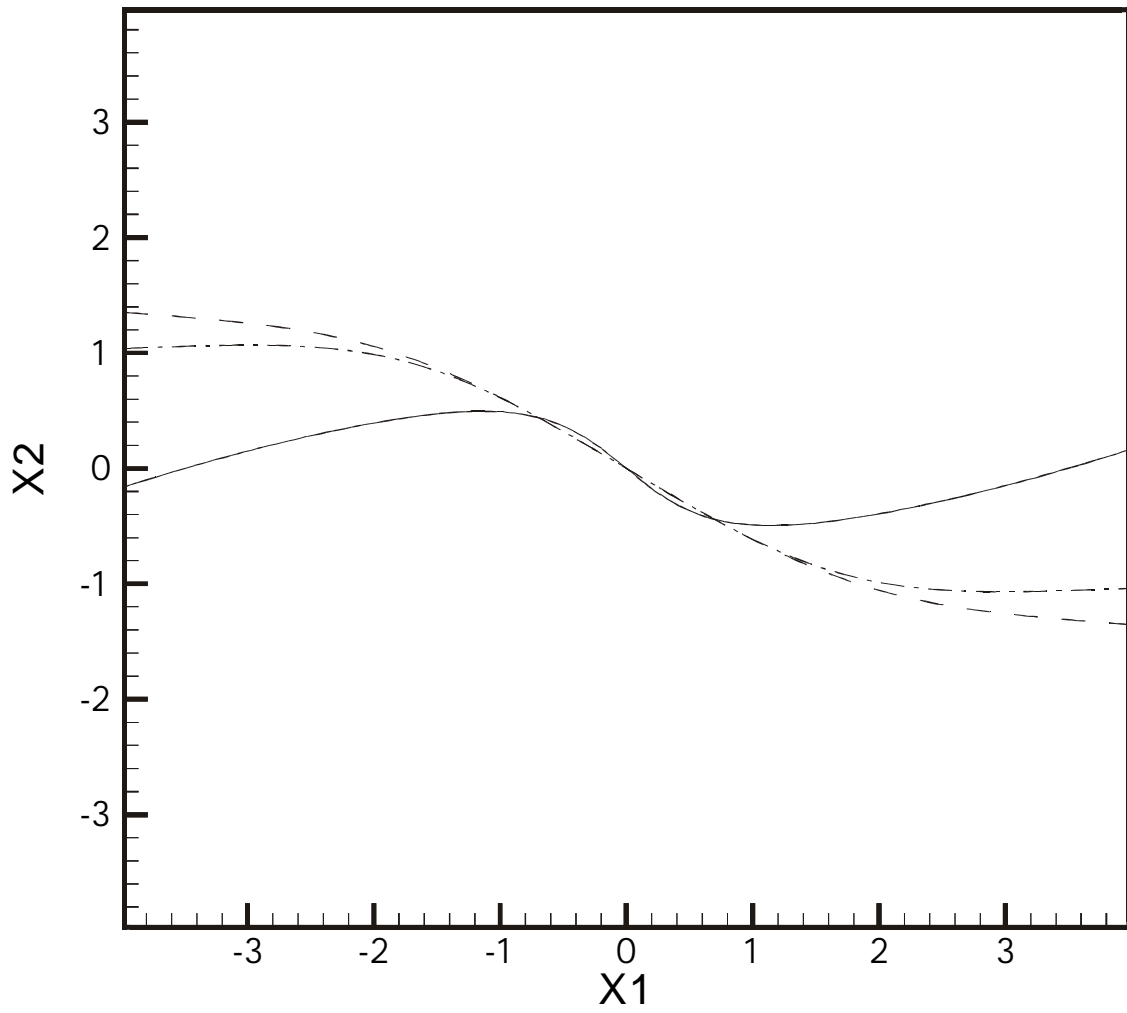


Figure 8. Comparison of switching lines for Mayer, Lagrange and Boltz cost functions.

Solid – the Mayer cost function, Dashed – the Lagrange cost function, Dash-dot – the Boltz cost function at $\tau = \pi$.

2.5 Multi-Degree-of-Freedom System with terminal cost function

For problems considered in Sections (2.2) and (2.3), equation of motion of dynamic system is linear. Therefore, it seems reasonable to try to extend the ‘hybrid’ solution method to the case of multi-degree-of-freedom systems.

2.5.1 Problem statement

Consider a randomly excited controlled system with n degrees of freedom, governed by the matrix equation of motion (Bratus et. al., 2000)

$$M\ddot{X} + KX = U(t) + B(t)\zeta(t) \quad (2.40)$$

Here $X(t)$ and $U(t)$ are now n -dimensional column vectors of displacements and control forces respectively, with components $x_i(t)$ and $u_i(t)$, $i = 1, \dots, n$; M and K are symmetric positively definite $n \times n$ – matrices of masses and stiffnesses respectively, $\zeta(t)$ is a vector of independent random Gaussian white noises with unit intensities; $B(t) = \|b_{ij}(t)\|$; $i, j = 1, 2, \dots, n$. (Just for brevity the original control forces, as well as transformed control forces – components of vectors U and V respectively – are shown here as functions of time only, whereas for a system with feedback control they may depend on all system’s state variables). The following bounds are imposed on the possible magnitudes of control forces:

$$U(t) \in S_R, \text{ where } S_R = \{u_i(t) : |u_i| \leq R_i, i = 1, \dots, n\}, R_i > 0 \quad (2.41)$$

The total response energy at time instant t is $W = (1/2)[(M\dot{X}, \dot{X}) + (KX, X)]$, where parenthesis denotes dot product of vectors. The matrices of mass and stiffness can be diagonalized by a nonsingular transformation with $n \times n$ -matrix $A = \|a_{ij}\|, i, j = 1, \dots, n$, such that

$$A^T M A = I, \quad A^T K A = \Omega^2 \quad (2.42)$$

Here I is the identity matrix, whereas matrix Ω^2 is diagonal with elements $\Omega_i^2, i = 1, \dots, n$, and superscript “ T ” denotes transposal. Furthermore, A may be represented as a product of an orthogonal matrix Q and a certain diagonal matrix. Introducing now modal coordinates (Meirovitch L. 1986) as $Y = A^{-1}X$ and using the relations (2.42), the equation of motion (2.40) and the expression for energy are reduced respectively to

$$\ddot{Y} + \Omega^2 Y = A^T U(t) + A^T B(t)\xi(t) \quad (2.43)$$

$$W = (1/2)[(\dot{Y}, \dot{Y}) + (\Omega^2 Y, Y)] = (1/2) \sum_{i=1}^n [\dot{y}_i^2(t) + \Omega_i^2 y_i^2(t)] \quad (2.44)$$

In view of inequalities (2.41) the column vector $V(t)$ of transformed control forces, with components

$$v_i(t) = \sum_{j=1}^n a_{ji} u_j(t) \quad (2.45)$$

belongs to a set

$$S_\rho = \{v_i(t) : |v_i(t)| \leq \rho_i, i = 1, 2, \dots, n\}, \rho_i = \sum_{j=1}^n |a_{ji}| R_j \quad (2.46)$$

The transformed equation (2.43) may be rewritten in a space state (scalar) form as

$$\begin{aligned} \dot{y}_i &= p_i, \dot{p}_i = -\Omega_i^2 y_i + v_i + \xi_i(t), \quad i = 1, 2, \dots, n \\ \xi_i(t) &= \sum_{k=1}^n \sigma_{ki}(t) \xi_k(t), \quad \sigma_{ki}(t) = \sum_{j=1}^n a_{ji} b_{jk}(t) \end{aligned} \quad (2.47)$$

Introducing “backward” time $\tau = t_f - t$, the HJB equation for H can be written as

$$\partial H / \partial \tau = \sum_{i=1}^n \left[p_i (\partial H / \partial y_i) - \Omega_i^2 y_i (\partial H / \partial p_i) - \rho_i |\partial H / \partial p_i| \right] + (1/2) \text{Tr}(\sigma \sigma^T H_{pp}) \quad (2.48)$$

the initial condition being

$$H(Y, P, 0) = (1/2) \sum_{i=1}^n (\Omega_i^2 y_i^2 + p_i^2) \quad (2.49)$$

Here σ and H_{pp} are $n \times n$ – matrices of σ_{ij} and $\partial^2 H / (\partial p_i \partial p_j)$ respectively, whereas terms with ρ_i in the HJB equation (2.48) appear due to minimizing over v_i of the original terms with $v_i (\partial H / \partial p_i)$. This minimization, in view of the inequalities (2.46), yields

$$v_i = -\rho_i \operatorname{sgn}(\partial H / \partial p_i), \quad \operatorname{sgn} z = +1 \text{ for } z > 0, \operatorname{sgn} z = -1 \text{ for } z < 0 \quad (2.50)$$

2.5.2 Analytical Solution to the HJB Equation for an “outer” domain

It can be verified, by direct substitution, that the function

$$\begin{aligned} H(Y, P, \tau) = & (1/2) \sum_{i=1}^n \left\{ \left[p_i - (\rho_i z_i / \Omega_i) \sin \Omega_i \tau \right]^2 + \left[\Omega_i y_i + (\rho_i z_i / \Omega_i) (1 - \cos \Omega_i \tau) \right]^2 \right\} + \\ & (1/2) \sum_{k=1}^n \sum_{i=1}^n \int_0^\tau \sigma_{ik}^2 (T - s) ds \\ z_i = & \operatorname{sgn} \left[(\rho_i \operatorname{sgn} p_i - (\rho_i / \Omega_i) \sin \Omega_i \tau) \operatorname{sgn} p_i \right] \end{aligned} \quad (2.51)$$

is the solution to the problem (2.48), (2.49) within domain

$$\mathbf{D} = \bigcup_{i=1}^n \mathbf{D}_i; \quad \mathbf{D}_i = \{Y, P, \tau : |p_i| > (\rho_i / \Omega_i) |\sin \Omega_i \tau|\}, \quad i = 1, 2, \dots, n \quad (2.52)$$

Indeed, substituting the expression (2.51) for H into the PDE (2.48) yields the equation

$$\sum_{i=1}^n (\rho_i^2 / \Omega_i) \sin \Omega_i \tau = \sum_{i=1}^n \rho_i [p_i z_i - |p_i - (\rho_i z_i / \Omega_i) \sin \Omega_i \tau|]$$

which would be certainly satisfied if it is satisfied simultaneously, term by term, for every i . Thus, the proof is reduced to the previously considered one for a SDOF system. The optimal control law within the domain D is found to be

$$\begin{aligned} v_i(\tau)^* &= -\rho_i \text{ for } (Y, P, \tau) \in \mathbf{D}_i^+, \mathbf{D}_i^+ = \{Y, P, \tau : p_i > (\rho_i / \Omega_i) |\sin \Omega_i \tau|\} \\ v_i(\tau)^* &= \rho_i \text{ for } (Y, P, \tau) \in \mathbf{D}_i^-, \mathbf{D}_i^- = \{Y, P, \tau : p_i < -(\rho_i / \Omega_i) |\sin \Omega_i \tau|\} \end{aligned} \quad (2.53)$$

which is clearly seen to be the dry-friction law for the i -th DOF. Thus, as in the case of SDOF, this law differs from the perfectly optimal one within the “inner” domain only.

The above analysis provides a complete solution to the problem of optimal control, as long as the required control forces for transformed, or modal coordinates (vector $V(t)$) can be implemented indeed. In certain applications this may not be the case, and one should generate vector $U(t)$ of the control forces, applied to the original coordinates. Then one should resolve – for every point of the state space and every time instant - the set of linear algebraic equations (2.45) in terms of $u_j(t)$, where $v_i(t_f - t)$ are optimal control forces, as governed by relations (2.50). The natural question arises then: will the resulting original control forces – components of the vector U - satisfy the original bounds (2.41)? Regretfully, the answer is negative in general, the reason being nonlinear operation of maximization, which “sneaks in” between direct modal transformation $Y = A^{-1}X$ and its inverse.

To illustrate this effect and outline the proposed procedure for generating a reasonable control strategy consider first a simple case of two DOFs ($n = 2$). Let a primary mass be attached to a rigid base via primary elastic spring, and a secondary mass be attached to the primary one via secondary spring. Then, using subscripts 1 and 2 respectively for primary and secondary masses/stiffnesses, as well as for their displacements and corresponding control forces, the matrix equation of motion (2.40) may be written, with

$$M = \begin{bmatrix} m_1 & 0 \\ 0 & m_2 \end{bmatrix}, K = \begin{bmatrix} k_1 + k_2 & -k_2 \\ -k_2 & k_2 \end{bmatrix} \quad (2.54)$$

The matrix A, which transforms the system to the form (2.43), may be written as

$$A = \begin{bmatrix} -m_1^{-1/2} \sin \alpha & m_1^{-1/2} \cos \alpha \\ m_2^{-1/2} \cos \alpha & m_2^{-1/2} \sin \alpha \end{bmatrix} \quad (2.55)$$

$$\alpha = \tan^{-1} \left[\left(k_1 + \sqrt{4k_2^2 + k_1^2} \right) / k_2 \right]$$

This results in the transformed equations (2.47) with

$$\Omega_i^2 = \lambda_i / m_i, i = 1, 2, \lambda_{1,2} = (1/2) \left(2k_2 + k_1 \pm \sqrt{4k_2^2 + k_1^2} \right) \quad (2.56)$$

These explicit expressions for elements of the matrix A in terms of original masses and stiffnesses should be used in the equations (2.45) and (2.46) for the transformed control forces and their bounds respectively.

It can be seen that only four pairs of optimal values of the transformed control forces are possible, namely $v_1^* = \pm \rho_1, v_2^* = \pm \rho_2$, with different combinations of positive and negative signs within various domains of space state and time (the optimal values are denoted here by star superscripts, which will also be used for the optimized original control forces). Resolving relations (2.45) in terms of the original control forces for each of the above combinations of signs (with coefficients as defined by expressions (2.55)) yields

$$\begin{aligned}
& \text{Cases } A, D : v_1^* = \pm \rho_1, v_2^* = \pm \rho_2 \Rightarrow \\
& u_1^* = \pm R_1 (|\cos \alpha| \cos \alpha - |\sin \alpha| \sin \alpha) \pm R_2 (|\sin \alpha| \cos \alpha - |\cos \alpha| \sin \alpha), \\
& u_2^* = \pm R_1 (|\sin \alpha| \cos \alpha + |\cos \alpha| \sin \alpha) \pm R_2 (|\cos \alpha| \cos \alpha + |\sin \alpha| \sin \alpha) \\
& \text{Case } B : v_1^* = -\rho_1, v_2^* = \rho_2 \Rightarrow \\
& u_1^* = R_1 (|\sin \alpha| \sin \alpha + |\cos \alpha| \cos \alpha) + R_2 (|\cos \alpha| \sin \alpha + |\sin \alpha| \cos \alpha) \\
& u_2^* = R_1 (|\cos \alpha| \sin \alpha - |\sin \alpha| \cos \alpha) + R_2 (|\sin \alpha| \sin \alpha - |\cos \alpha| \cos \alpha) \\
& \text{Case } C : v_1^* = \rho_1, v_2^* = -\rho_2 \Rightarrow \\
& u_1^* = -R_1 (|\sin \alpha| \sin \alpha + |\cos \alpha| \cos \alpha) - R_2 (|\cos \alpha| \sin \alpha + |\sin \alpha| \cos \alpha) \\
& u_2^* = R_1 (|\sin \alpha| \cos \alpha - |\cos \alpha| \sin \alpha) + R_2 (|\cos \alpha| \cos \alpha - |\sin \alpha| \sin \alpha)
\end{aligned} \tag{2.57}$$

The resulting four pairs of values u_1^*, u_2^* define four points on the u_1, u_2 plane. We may denote them as A, B, C and D, using the same notation as for the corresponding cases as defined by the expressions (2.57) (with the upper (plus) sign being used for the case A in the double-sign expression, and lower (minus) - for the case D).

STATEMENT 3. The quadrangle ABDC is a rectangle, circumscribed around the rectangle $|u_1| \leq R_1, |u_2| \leq R_2$ (see Figure 9).

To prove that vectors, say, \overrightarrow{AB} and \overrightarrow{CD} are collinear one can directly compare their angles by calculating, from expressions (2.57), relevant differences in coordinates

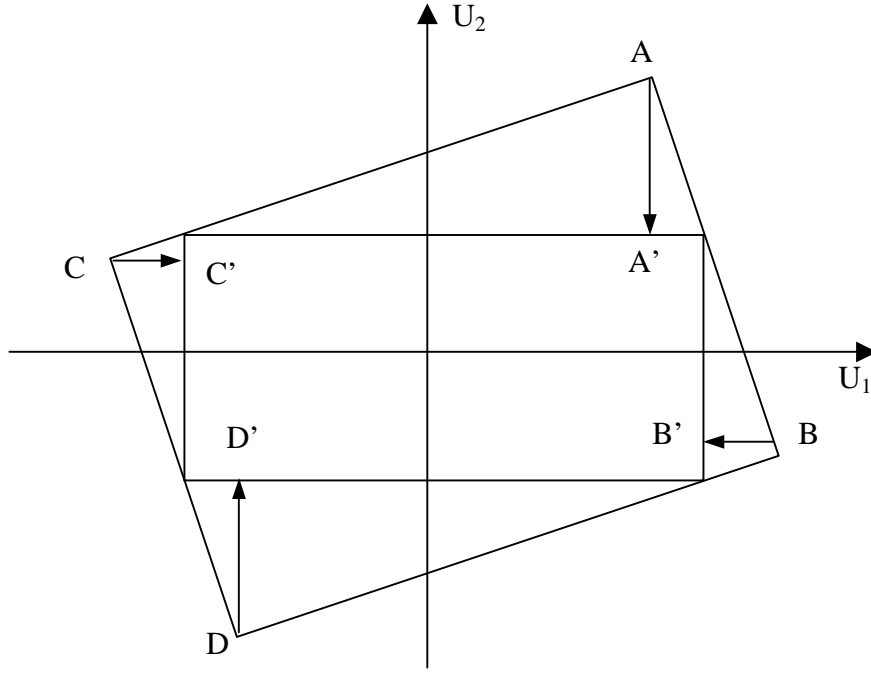


Figure 9. Optimal transformed control forces on a plane u_1, u_2 of the original control forces for a TDOF system

first between points A and B and then between points C and D. Similarly, it can be shown that vectors, say, \overrightarrow{AB} and \overrightarrow{BD} are orthogonal, whereas \overrightarrow{AC} and \overrightarrow{BD} are collinear.

Consider now, for definiteness, the case, where $0 \leq \alpha \leq \pi/2$. The equation of the straight line AB is then found to be

$$\frac{u_1 - R_1 \cos 2\alpha}{R_1(1 - \cos 2\alpha) + R_2 \sin 2\alpha} = \frac{u_2 - R_1 \sin 2\alpha + R_2}{-R_2(1 + \cos 2\alpha) - R_1 \sin 2\alpha}$$

and it is clearly satisfied by the pair $u_1 = R_1, u_2 = R_2$. It can be shown similarly, that $(R_1, -R_2) \in BD, (-R_1, -R_2) \in CD, (-R_1, R_2) \in CA$. Figure 10. illustrates positions of the rectangle ABDC for several values of α and $R_1 = 2, R_2 = 1$.

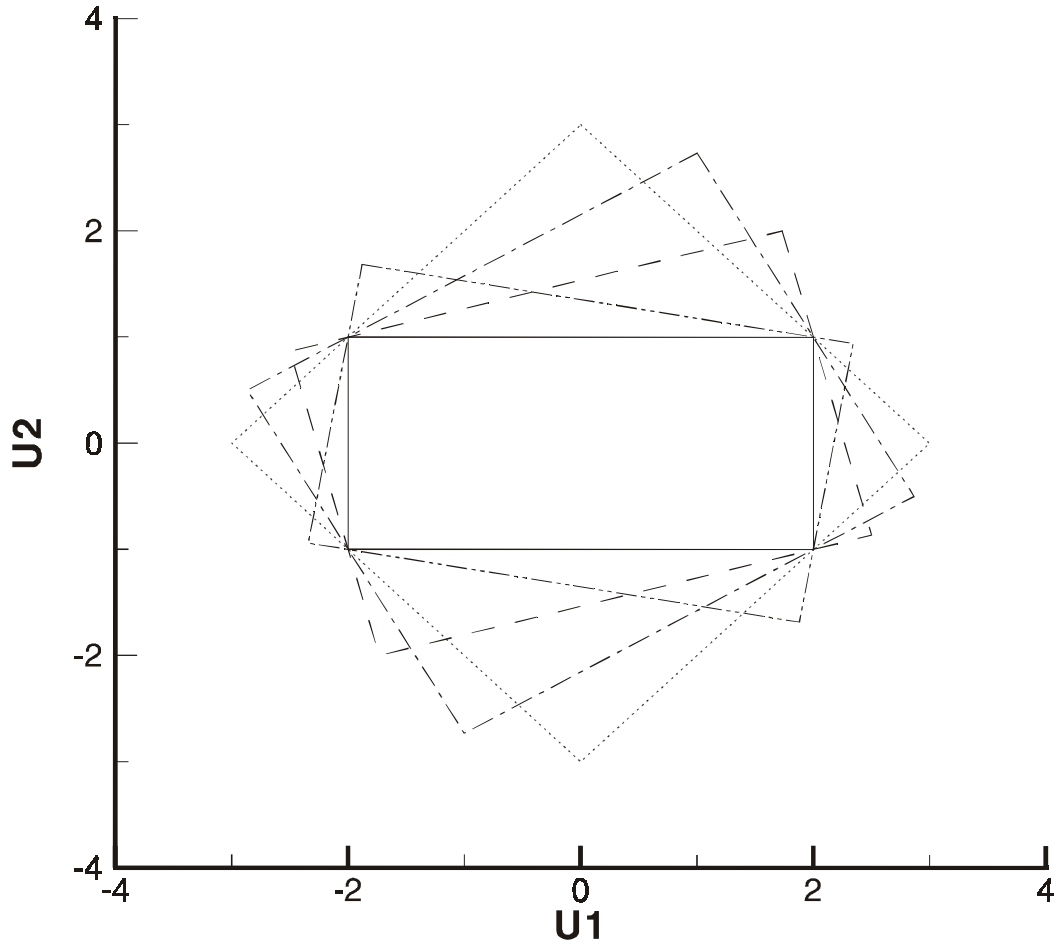


Figure 10. Optimal transformed control forces for various stiffness ratios, as represented by the corresponding values of the angle α (in degrees): 0 – solid, 15 – dashed, 30 – dash-dot, 45 – dotted, 80 – dash-dot-dot.

This example shows clearly, that any pair of possible values of the optimal transformed control forces v_1^*, v_2^* corresponds to such a pair of the original control forces u_1^*, u_2^* , that one of the conditions (2.41) is always satisfied whereas the other one is always violated. For example, $0 < u_1 < R_1 = 2, u_2 > R_2 = 1$ for the highest corner point of the dashed rectangle in Figure 10 ($\alpha = 15^\circ$). A reasonable way to handle this problem is to project the apexes of the rectangle ABDC onto the nearest sides of the rectangle $|u_1| \leq R_1, |u_2| \leq R_2$. These projections are denoted in Figure 9 by the same letters with primes. The resulting control laws may be called “semioptimal” – literally (!), since one of the forces is kept at its optimal value, whereas the other one is reduced in magnitude in order to comply with the relevant bound (2.41). And this reduction is made along the shortest route on the plane of control forces.

This simple example illustrates the approach, which is suggested for a general MDOF system with an arbitrary n . Let $u_j^*, j = 1, 2, \dots, n$ be solution to the equation set (2.45) for the corresponding domain Y, P, τ . Denote by J^+ and J^- lists of those indices j , for which, respectively, $u_j^* > R_j$ and $u_j^* < -R_j$. The “semioptimal” control law, which may be suggested then for this domain, is as follows (it is denoted by adding bars)

$$\bar{u}_j^* = +R_j \text{ for } j \in J^+; \bar{u}_j^* = -R_j \text{ for } j \in J^-; \bar{u}_j^* = u_j^* \text{ for } j \notin J^+ \cup J^- \quad (2.58)$$

2.6 Multi-Degree-of-Freedom System with integral cost function

2.6.1 Problem statement

Consider now the case of integral cost functional for the system (2.43), by introducing the following multidimensional counterpart of the Bellman S-function in transformed state variables

$$S = (1/2) \min_u \mathbb{E} \int_t^{t_f} \sum_{i=1}^n (p_i^2 + \Omega_i^2 y_i^2) dt \quad (2.59)$$

The corresponding HJB equation, similar to one for SDOF (2.30) is then

$$\begin{aligned} \partial S / \partial \tau = & \sum_{i=1}^n \left[p_i (\partial S / \partial y_i) - \Omega_i^2 y_i (\partial S / \partial p_i) - \rho_i |\partial S / \partial p_i| + (1/2) (p_i^2 + \Omega_i^2 y_i^2) \right] \\ & + (1/2) \text{Tr}(\sigma \sigma^T S_{pp}) \end{aligned} \quad (2.60)$$

2.6.2 Analytical Solution to the HJB Equation for an “outer” domain

Consider now equation (2.60) with the initial condition $S(Y, P, 0) = 0$. The following function

$$\begin{aligned} S(Y, P, \tau) = & \sum_{i=1}^n \left\{ \frac{1}{2} (\Omega_i^2 y_i^2 + p_i^2) \tau + \frac{\rho_i z_i}{\Omega_i^2} [\Omega_i^2 y_i \tau + p_i (\cos \Omega_i \tau - 1) - \Omega_i y_i \sin \Omega_i \tau] \right\} + \\ & \sum_{i=1}^n (\rho_i / \Omega_i)^2 (\tau - \Omega_i^{-1} \sin \Omega_i \tau) + (1/2) \sum_{i=1}^n \sum_{k=1}^n \sigma_{ik}^2 (T - s) s ds; \quad z_i = \text{sgn } p_i, i = 1, 2, \dots, n \end{aligned} \quad (2.61)$$

provides the solution to the corresponding HJB equation (2.60) within the “outer” domain

$$\mathbf{D} = \bigcup_{i=1}^n \mathbf{D}_i; \quad \mathbf{D}_i = \{Y, P, \tau : |p_i \tau| > (\rho_i z_i / \Omega_i^2) \cos \Omega_i \tau - 1\} \quad (2.62)$$

The optimal control law within the domain (2.62) is found to be, similarly to the SDOF case, the dry-friction law

$$v_i = -\rho_i \operatorname{sgn}(\partial S / \partial p_i) = -\rho_i \operatorname{sgn} p_i, \quad i = 1, 2, \dots, n$$

Numerical solution to this type of problems represents tremendous difficulties, because the multidimensional HJB equation has to be solved. However, for integral cost function, similar to the case for a SDOF system, it is easy to show that with τ increasing, the “outer” domain will expand everywhere but lines $p_i = 0, i = 1, 2, \dots, n$. Thus, it seems reasonable to apply simple dry friction control law, as long as in this case there is no need to solve this multidimensional HJB equation. For the terminal cost function, however, a certain inaccuracy will always exist in this case, which may be estimated from the case of SDOF system, explained in Section 2.3.2.

2.7 Dry friction is the optimal control law for steady-state response

In many potential applications of active vibration control systems (such as in earthquake engineering, for shipboard and offshore equipment in rough seas, etc.) the main objective may be just to reduce the level of sustained vibrations. Therefore, a special study seems worthwhile for the case of a steady-state response, which is established after the (asymptotically stable) controlled system “forgets” its initial state. The complete “hybrid” analysis, as described above, seems to be very difficult for this case, as long as it requires marching in time with numerical solution of the HJB equation up to very large times. On the other hand, study of this special case can be made using just the analytical solution (2.32) if the integral cost functional is used as the optimization criterion. The solution shows the simple dry-friction control law to be optimal for this case of a “long-term control”. Certain estimates of the overall response level are obtained also in this section for the case of constant intensity of the white-noise excitation, where the steady-state response is stationary as well. This is done both by direct energy balance analysis through application of the SDE Calculus and by the stochastic averaging method, which is used to obtain certain reliability estimates for the optimally controlled system.

Substituting the solution (2.32) into the expression (2.29) yields

$$u = -R \operatorname{sgn} x_2 = -R \operatorname{sgn} \dot{x} \quad (2.63)$$

thereby showing the simple dry-friction control law to be optimal now within the outer domain. This domain is clearly expanding with increasing the “backward” time $\tau = t_f - t$, and with $\tau \rightarrow \infty$ the inner domain – one where the opposite one to the inequality (2.31) holds – shrinks down to the x_2 – axis. *This means that the control law (2.63) is the optimal one for “long-term” control of the steady-state response, irrespectively of the magnitudes of the excitation intensity and/or bound for the control force.* This result may be directly extended to MDOF systems with Lagrange cost function, as long as a mean system’s energy is a subject to be minimized. This result is extremely important, because no numerical simulation to the HJB equation, which is one of the most difficult and time consuming part of optimal control problems, is needed at all.

2.8 Conclusions

The Hybrid solution method for the HJB equations proved itself to be an efficient approach to optimal bounded control of random vibrations. The essential part of the approach is an analytical solution within a certain “outer” domain of the phase plane for SDOF systems. The solution provides both optimized values of the cost functional (of the response energy in this work) and the optimal control law; the latter has been found to be just a simple “dry-friction” law in this work. The analytical solution is supplemented by the numerical one within the remaining inner domain, and provides boundary conditions for the latter, thereby being of great help for developing the complete hybrid solution.

The numerical solution provides switching lines (surfaces) within inner domains, which correspond to the desired optimal “bang-bang” control. For a special case of so-called “long-term” control (integral cost functional of a steady-state response) the dry-friction control is shown to be the optimal one within the whole phase plane. The above solutions to problems of optimal control have been extended to MDOF systems, using transformation to modal coordinates.

3. Nonlinear random vibrations of Piecewise Conservative systems

In this Chapter a new name will be introduced for a certain type of nonlinear systems. This type of systems appears as a result of application of optimal bounded in magnitude control force. Analysis of motion of such type of system is to be profoundly described by means of a newly developed Energy Balance method. Analytical results, obtained with the Energy Balance method will be compared with results of numerical simulation of governing equation of motion.

3.1 Piecewise Conservative systems

Study of nonlinear systems is much more difficult than that of linear systems. For the latter principle of superposition holds, which significantly simplify a way of finding solution. There is no such thing as superposition principle for nonlinear systems and therefore each nonlinear system has to be treated in its own way. There are several well-known methods developed for treating nonlinear systems, such as averaging methods (Dimentberg 1988, Lin et. al. 1995), perturbational approach and others.

However, there are some categories, which nonlinear systems are divided into, based on system's properties usually. Each of these categories may have its own best way of finding solution. For example, a system which stiffness characteristics consist of several continuously connected linear parts is usually called as a piecewise linear one. A

quasiconservative system is a system, for which an amount of input energy due to external excitation is approximately equal to the amount of energy, absorbed by some damping mechanism. Lets now consider a new name for a certain nonlinear system, namely (Iourtchenko et. al., 2000)

DEFINITION 1. Nonlinear vibratory systems with stepwise finite energy losses, which appear at discrete time instants only are called piecewise conservative one.

Typical example of such a system is a vibroimpact system with dominant mechanism of energy loss being impacts with imperfect rebounds. It is clear that system is conservative always except for instant of impact. Another example is a system with externally imposed instantaneous stepwise variations, or “jumps”, of parameters, which can either bring in or carry away the system’s energy (pendulum clocks, swings, etc.). It may be added, that certain non-conservative systems may be treated as the piecewise-conservative ones. An example is a SDOF system with dry friction, or resistance force of a constant magnitude with its direction being always opposite to that of the system’s velocity. By including work of this force into the system’s total energy, one can describe energy losses in vibration as being instantaneous, corresponding to reversals of velocity. The described kind of phenomena may also be observed in systems with active control of a “bang-bang” type, whereby the available control force, as developed by an actuator, is of a bounded magnitude; the optimal bounded control law is usually obtained as a sequence of “switches” between the given bounds.

3.2 Energy Balance Method

These types of energy losses make the vibrating systems nonlinear in general, as long as the instants of stepwise variations aren't known in advance but rather are governed by the equations of motion. This nonlinearity greatly complicates analyses of the systems' response to a random excitation. Even for a SDOF system such an analysis requires either use of some moment closure scheme, or use of the stochastic averaging approach, which is valid only for small energy losses and excitation intensity.

An alternative method for response prediction is proposed here for a SDOF system, subjected to a white-noise excitation. The method is based on a direct balance of the expected response energy and therefore is called a Direct Energy Balance method. A stochastic differential equation (SDE) for the total response energy $E(t)$ is derived from the original equation of motion. A conditional averaging is first applied to this SDE, denoted by bar, the condition being initial value of E at the start of a certain response cycle. This results in the deterministic ODE $\bar{\dot{E}} = D/2$, with D being intensity of the white-noise excitation, thereby implying linear growth of the (conditional) expected response energy with time. After deducting properly evaluated energy loss within the cycle, the conditional expectation of energy at the start of the next cycle can be evaluated. (The actual value of energy at this instant will be random). The concept of a "cycle" is problem-dependent, of course, but it is unambiguously defined by finite relation(s), which control the instantaneous energy losses. Thus, in case of a vibroimpact system with a single rigid barrier the cycle corresponds to a time interval between two consecutive rebounds (or impacts).

The above procedure results in a random sequence of values of E at the starting instants of various cycles. The unconditional averaging is applied then to this sequence, i.e. averaging over all response cycles, as denoted by angular brackets. As long as a stationary sequence has a constant mean value, the mean net energy increment per cycle should be zero. This results in a simple energy balance relation

$$\langle \Delta E \rangle = DT/2 \quad (3.1)$$

where the LHS is a total mean energy loss per cycle. It is related to the system's energy and/or other state variables by a specific equation for energy loss for a given problem. The RHS is a mean energy input per cycle, with T being expected duration of the cycle. It can be identified as a solution to the relevant first-passage problem for the response – namely as an expected time to arrive at the starting point of the next response cycle after start of the present cycle with energy E . This (conditionally) expected time satisfies the relevant generalized Pontryagin equation (Lin et. al., 1995), which had been identified and analyzed in (Dimentberg et. al., 1999) for the corresponding vibroimpact system. Solution $T(H)$ to this PDE, which is to be used in the exact (by itself) relation (3.1), with E replaced by its unconditional mean value, is the challenging part of the approach. It may be added, that in general T may also be present in the LHS of the relation (3.1); this will be the case where the magnitude of the energy drop depends not only, say, on the initial energy of the cycle, but on the instantaneous energy as well.

It will be shown later that, a perturbational analysis of the second-order PDE for $T(E)$ has been made in (Dimentberg et. al., 1999), with excitation intensity D regarded

as a small parameter. In a zero-order approximation, $D = 0$, the PDE is of the reduced (first) order, and its exact solution is just the system's natural half-period, or $T = \pi/\Omega$, where Ω is the system's natural frequency. As long as the solution satisfies both boundary conditions for the original PDE, this is the case of regular rather than singular perturbations. Thus, the solution for the deterministic cycle duration T of the system without excitation may naturally be used in the relation (3.1). Relying on the above analysis for a vibratory system, a cycle duration time T will be taken as a system's natural period in all example problems considered below. Of course, this would imply that the predictions are approximate only for not-very-small D 's. It may be speculated, however, that their accuracy should be higher than that of the asymptotic stochastic averaging – simply because the latter requires not only small variations of the response period, but also small variations of the response energy per cycle (and thus, small losses). This general expectation had been confirmed in (Dimentberg et. al., 1999) for a vibroimpact system by results of a direct Monte-Carlo simulation.

Thus, the Energy Balance approach may provide better accuracy than the asymptotic one whenever the system's losses and excitation level are not very small, and a single expected value of a certain response characteristic is adequate for a given application – for example, to evaluate efficiency of a “bang-bang” control. The type of response characteristic to be obtained from the relation (3.1) is problem-dependent. For example, expected response energy is predicted in four of five specific problems considered in this paper, whereas expected response amplitude, or peak value of the displacement, is predicted in the fifth one. The superior accuracy of the energy balance approach is demonstrated, by direct Monte-Carlo simulation, for all these problems:

relation (3.1) is shown to provide reasonable results far beyond the applicability range of the stochastic averaging.

Possibility for extending this approach to systems with nonlinear restoring forces should be also mentioned here. Introducing relevant potential energy function, one can obtain the same linear growth law for the corresponding total energy, leading eventually to the same energy balance equation (3.1) for the steady-state response. The difference for the nonlinear case is in the RHS of this equation, where T should now depend on H , that is, on instantaneous starting energy value of the response cycle, even if it is predicted approximately as the natural cycle duration for a system without random excitation. For a slightly nonlinear system with smooth nonlinearity, with $T(E)$ being linear in E , the linear part may be included into the RHS of the equation (3.1), together with the constant one. As long as the energy loss in the LHS depends on the same E , the mean response energy can be predicted indeed (In general, however, the functions of E in two sides of the equation (3.1) may appear to be different, thereby precluding the desired estimate without independent information on the relation between these functions).

3.3 Piecewise Conservative systems - vibroimpact system

3.3.1 Application of Energy Balance method

Consider a SDOF mass-spring system, with a rigid barrier installed with an offset h from the system's static equilibrium position. The equations of motion between impacts may then be written as

$$\dot{y} = v, \dot{v} = -\Omega^2 y + \zeta(t), \text{ for } y > -h \quad (3.2)$$

Thus, positive and negative values of h may imply, say, pretension and slack respectively in the mooring line of a floating moored body. The excitation $\zeta(t)$ is assumed here, as well as in all other examples to be a zero-mean stationary Gaussian random white noise, with intensity denoted by D . The impact/rebound condition, which should be satisfied at time instants t_* , when $y = -h$, may be written, by introducing restitution factor r , as

$$v_+ = -rv_-; v_{\pm} = v(t_* \pm 0); y(t_*) = -h; 0 < r \leq 1 \quad (3.3)$$

According to the Energy Balance method (Section 3.2) lets introduce total response energy $E(t)$ as

$$E = \dot{y}^2/2 + U(y), \quad U(y) = \Omega^2 y^2/2, \quad \dot{E} = \dot{y}(\ddot{y} + \Omega^2 y) = v\zeta(t) \quad (3.4)$$

and applying conditional averaging for a given $E(0)$, yields, according to the basic SDE calculus (Dimentberg 1988, Lin et. al., 1995)

$$\dot{\bar{E}} = D/2, \quad \bar{E}(t) = E(0) + Dt/2 \quad (3.5)$$

Energy evolution equation (3.5) may be applied to predict response energy at impact as well as conditional mean square impact velocity

$$\bar{E}(t_* - 0) = E(0) + Dt_*/2, \quad \bar{v}_-^2 = 2E(0) + Dt_* - 2E_*, \quad E_* = U(-h) = \Omega^2 h^2 / 2 \quad (3.6)$$

The impact/rebound condition (3.3) is applied now to obtain mean square rebound velocity and response energy after rebound – that is, at the start of the next cycle:

$$\bar{v}_+^2 = r^2 \bar{v}_-^2, \quad \bar{E}(t_* + 0) = r^2 [E(0) + Dt_*/2 - E_*] + E_* \quad (3.7)$$

The unconditional averaging as denoted by angular brackets is applied now to the relation (3.7). Imposing then stationarity condition for the expected energy at the start of a cycle yields the following reduced energy balance relation

$$\langle E(0) \rangle = \langle \bar{E}(T + 0) \rangle, \quad T = \langle t_* \rangle, \quad \langle E(0) \rangle = E_* + \frac{r^2 (DT/2)}{1 - r^2} \quad (3.8)$$

Unconditional mean square impact velocity can be found now, using equations (3.6) and (3.8), as

$$\langle v_-^2 \rangle = 2(E(0) - E_*) = DT / (1 - r^2) \quad (3.9)$$

This result is the same as obtained in (Dimentberg et al., 1999) for the case $h = 0$. Of course, in general the offset of the barrier h cannot but influence the response through the value of T . The cycle duration T in this work is approximated by the system's natural period. The latter can be easily obtained from the equation (3.2) with $\zeta(t) \equiv 0$ as

$$T(H) = \pi/\Omega + (2/\Omega)\sin^{-1}\sqrt{H_*/H} = \pi/\Omega + (2/\Omega)\sin^{-1}(\Omega h/\sqrt{2H}) \quad (3.10)$$

Thus, the solution (3.9) is meaningful for sufficiently small h only, which lead to negligibly small variations of T due to second term in the expression (3.10). Thus, the system (3.2), (3.3) should be quasiisochronous, although it should still be regarded as a strongly nonlinear one.

It is interesting to compare the “exact” mean square velocity (3.9) (quotation marks are applied since the exact value of T isn't available at present) with its limiting value for the case of small impact losses, i.e.

$$\langle v_-^2 \rangle_{AS} = \lim_{r \rightarrow 1} \langle v_-^2 \rangle = DT/[2(1-r)] \quad (3.11)$$

The latter expression can also be obtained by applying asymptotic stochastic averaging method to the SDE (3.2) with impact condition (3.3), as described in (Dimentberg 1988). Therefore, it should be valid only for values of $1 - r$, proportional to a small parameter. Actually both “exact” and approximate solutions, (3.9) and (3.11) respectively, rely on approximation of the cycle duration by the system's natural period; therefore, they are based on assumption of small D , and thus (implicitly) on that of small impact losses.

However, Monte-Carlo simulations on Figure 11 for the case $h = 0$ demonstrated (Dimentberg et. al., 1999) good accuracy of the energy-balance approach down to values $r = 0.7$ (Actually, the expected response energy was predicted with a good accuracy by

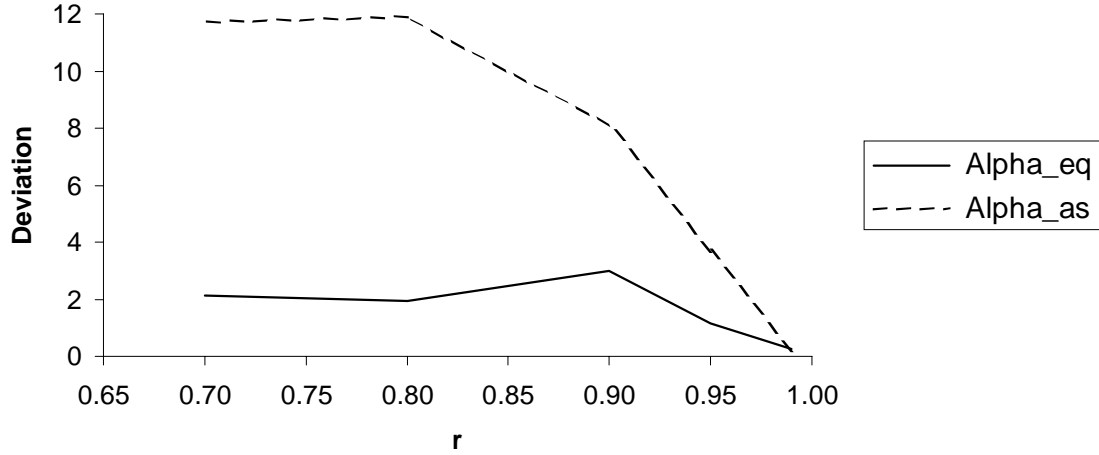


Figure 11. Absolute percent deviations of analytical result from numerical one.

Monte-Carlo simulation for different values of restitution factor r . Solid and dashed lines represent results, obtained with the use of α_{eq} and α_{as} respectively.

this approach with $T = \pi/\Omega$ even for $r = 0.6$, although the corresponding expected cycle duration was found to be rather lower than the natural period at so high level of impact losses). And they certainly were found to be superior to the asymptotic results for not-too-small values of $1 - r$. In other words, superior convergence rate of the energy-balance approach has been confirmed indeed, for this example, compared with the asymptotic approach, which requires small energy variations per cycle. Thus, in this example the energy-balance approach provides certain reasonably accurate predictions of the random response far beyond applicability range of the asymptotic stochastic averaging method.

To calculate a mean unconditional energy one has to take an average over a period from (3.5), which gives

$$E(t) = \frac{1}{T} \int_0^T \bar{E}(t) dt = \langle E(0) \rangle + DT/4 \quad (3.12)$$

This expression combining with (3.8) and $T = \pi/\Omega$ provides

$$E(t) = \frac{DT}{4} \left\{ \frac{1+r^2}{1-r^2} \right\} = \frac{D\pi}{4\Omega} \left\{ \frac{1+r^2}{1-r^2} \right\} \quad (3.13)$$

The derived formula (Dimentberg et. al 1999) for mean response energy may be used to obtain an improved “equivalent” viscous damping ratio. For this purpose, lets compare (3.13) with a value of mean energy of system with viscous or linear damping $E_{lin} = D/4\alpha$. Comparison will give the following value of equivalent damping coefficient

$$\alpha_{eq} = \frac{\Omega}{\pi} \left\{ \frac{1-r^2}{1+r^2} \right\} \quad (3.14)$$

3.3.2 Subharmonic response

This section is somehow related to the author’s Master Thesis, where a subharmonic response of a vibroimpact system has been considered. As long as the

improved formula for non-small impact losses has been established (3.14) for a very special system only, it seems natural to consider more general systems: with non-zero gaps and/or nonwhite excitation, MDOF systems, etc. The analytical study seems very difficult for these cases, as discussed in the previous sections. Therefore, a sort of a "brute-force" treatment can be attempted: a direct use of the formula (3.14) as a benchmark, with mandatory verification of the resulting predictions by Monte-Carlo simulation. Figure 12 illustrates such a benchmark use of the derived equivalent viscous damping factor for a much more complicated problem. A SDOF system, with a one-sided barrier, is excited by a (narrow-band) sinusoidal-in-time force with random phase modulation, and subharmonic response is considered. The barrier is slightly shifted from the system's equilibrium position, so that the equation of motion is

$$\ddot{y} + 2\alpha\dot{y} + \Omega^2 y = \lambda \sin \psi(t), \dot{\psi} = \nu + \sigma \xi(t) \text{ for } y > -h \quad (3.15)$$

whereas the impact condition (3.3) is imposed for $y = -h$ (where $y_1 = y, y_2 = \dot{y}$). Parameters $\lambda^2/2, \nu, \sigma^2/\nu$ represent, respectively, mean square value of the excitation, its expected or mean frequency and its relative bandwidth of power spectral density (PSD). For the case of small impact losses and small gap h the system (3.2) had been studied in author's Master Thesis, both analytically - by averaging over the period, and numerically. Actually, the following Zhuravlev transformation was used in [32,33] $y = |x| - h, \dot{y} = \dot{x} \operatorname{sgn} x$, which reduces the equation (3.15) to

$$\ddot{x} + 2\alpha\dot{x} + \Omega^2 x = h\Omega^2 \operatorname{sgn} x + \lambda (\operatorname{sgn} x) \sin \psi \quad (3.16)$$

and makes the jump in transformed velocity proportional to $1 - r$ (rather than to $1 + r$ as in (3.2)). The actual analysis was made for the case of elastic impact ($r = 1$), with understanding that the asymptotic equivalent viscous damping factor $(1 - r)(\pi/\Omega)$ can be added to the available one in equation (3.16), provided that $1 - r$ is small (the smallest value of r as used in (Dimentberg et. al., 1998) was $r = 0.9$).

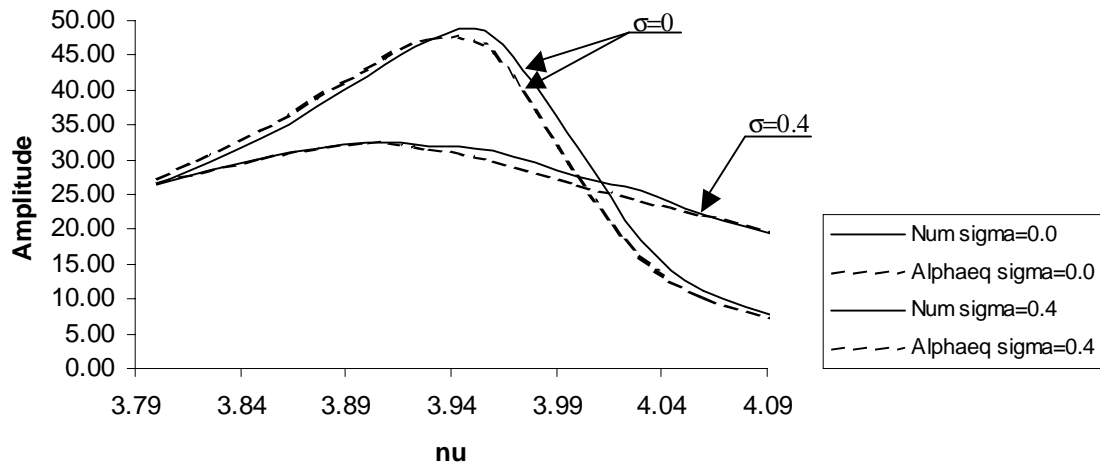


Figure 12. Application of α_{eq} for problem of subharmonic response.

Solid lines – with trace of impact $r = 0.8$, $\alpha = 0$, dashed lines – without trace of impact but $\alpha = \alpha_{eq} = 0.06987\Omega$

Figure 12 compares results of application of two different procedures for Monte-Carlo simulation for the case of subharmonic of the order $n = 2$, with mean excitation frequency being close to 4Ω . The first procedure used solution of the basic equation (3.15) with "honest" tracing of the impacts and imposing the impact condition (3.2) with

a given value of r ; viscous damping factor was assumed to be zero for these calculations and the results are represented by solid lines. The second procedure was based on numerical solution of the equation (3.16) - which is exactly equivalent to the original equation (3.15) in case of a perfectly elastic impact, or $r = 1$ - with $\alpha = \alpha_{eq}$, as calculated via formula (3.14) for the given r ; the results are represented by dashed lines. Frequency responses of the square root of mean square amplitude are presented in Figure 11 for cases of perfect and imperfect periodicity of the excitation ($\sigma = 0$ and $\sigma = 0.4$) and $r = 0.8$. The correlation between solid and dashed curves for the identical values of σ , corresponding to two different ways of accounting for impact losses, seem to be reasonable. It is clearly seen in particular, that use of the equivalent viscous damping model permits both qualitative and quantitative description of the basic effect - reduction of the peak subharmonic response amplitude with increasing excitation bandwidth, or random "disorder" in the periodic excitation.

3.3.3 Vibration of secondary structure

A problem of response of secondary mass is considered in this Section, when motion of the primary mass is described by equation (3.2) with impact condition (3.3). Such a "cascade" approximation (Dimentberg et. al., 1998) for the whole MDOF (nonlinear) vibroimpact system would be adequate at least in the case of small secondary/primary mass ratio. Motion of secondary mass may be expressed as

$$\ddot{z} + 2\alpha_s \dot{z} + \Omega_s^2 z = -\ddot{y} \quad (3.17)$$

with z being a relative motion. This approach permits to obtain analytical solution for the case of zero impact losses ($r = 1$) through the use of the following exact solution for autocorrelation function $K_{yy}(\tau)$ of stationary response $y(t)$ as obtained by (Dimentberg et al, 1998). The corresponding quadrature expression for power spectral density (PSD) $\Phi_{yy}(\omega)$ of $y(t)$ has been studied both numerically and analytically and used for predicting mean square response of a secondary structure; in particular, peaks of this PSD at $\omega = 2n\Omega, n = 1, 2, \dots$ were identified. Moreover, successive integration by parts in this expression yields the following asymptotic formula for the acceleration PSD at high frequencies:

$$\lim_{\omega \rightarrow \infty} \Phi_{\ddot{y}\ddot{y}}(\omega) = \lim_{\omega \rightarrow \infty} \omega^4 \Phi_{yy}(\omega) = (D/2\pi) Q \quad (3.18)$$

$$Q = 1 + 2\Omega/\pi\alpha$$

This limiting value of the PSD of base excitation is directly applicable in case of large Ω_s/Ω , with corresponding mean square response of the secondary mass being

$$\sigma_{z\infty}^2 = DQ/4\alpha_s^2\Omega_s^2 \quad (3.19)$$

Convergence rate to this high-frequency limit increases with primary damping ratio α/Ω . The case of inelastic impacts, or $r < 1$, will be addressed now. It should be noted, first of all, that the case of vanishingly small impact losses could be handled by asymptotic averaging over the period (Dimentberg 1988). Specifically, if value of $1 - r$ is proportional to a small parameter (is much smaller than unity), then these losses are

found to be equivalent to those due to viscous damping with the "asymptotically equivalent" factor $\alpha_{as} = (1-r)\Omega/\pi$. Of course, the resulting solution is approximate rather than exact. This equivalent viscous damping may be regarded as a "universal" one, valid for free vibration also.

However, for the random vibration problem at hand another formula for equivalent damping (3.14) may be more relevant, as derived by Energy Balance method through a direct analytical solution of the vibroimpact problem (with zero viscous damping) by the method of moments:

For the response of secondary structure the PSD of $y(t)$ is more relevant than its mean square value. Therefore, applicability of the improved formula (3.14) for incorporating the impact losses should be verified through Monte-Carlo simulations. The simulations were based on simultaneous numerical solution of the stochastic ODE (3.2) with $\alpha = 0$ together with impact condition and the following ODE for absolute displacement of secondary mass $x(t) = z(t) + y(t)$, as derived from the ODE (3.17):

$$\ddot{x} + 2\alpha_s \dot{x} + \Omega_s^2 x = -2\alpha_s \dot{y} - \Omega_s^2 y \quad (3.20)$$

To compare the results with predictions via formulae (3.18), (3.19) the assigned values of the restitution factor r were calculated according to the relation (3.14). Damping ratio of the secondary mass has been $\alpha_s/\Omega_s = 0.01$ throughout all simulation runs.

Figure 13 illustrates high accuracy of the asymptotic expression (3.19) with "impact magnification factor" Q as calculated via formula (3.18) by using expression (3.14) for equivalent damping, down to rather low value of the restitution factor $r = 0.72$.

The limiting condition for Monte-Carlo simulations used to be established from analytical data as presented in (Dimentberg et al 1998); for this specific case the corresponding natural frequencies ratio was $\Omega_s/\Omega=12$.

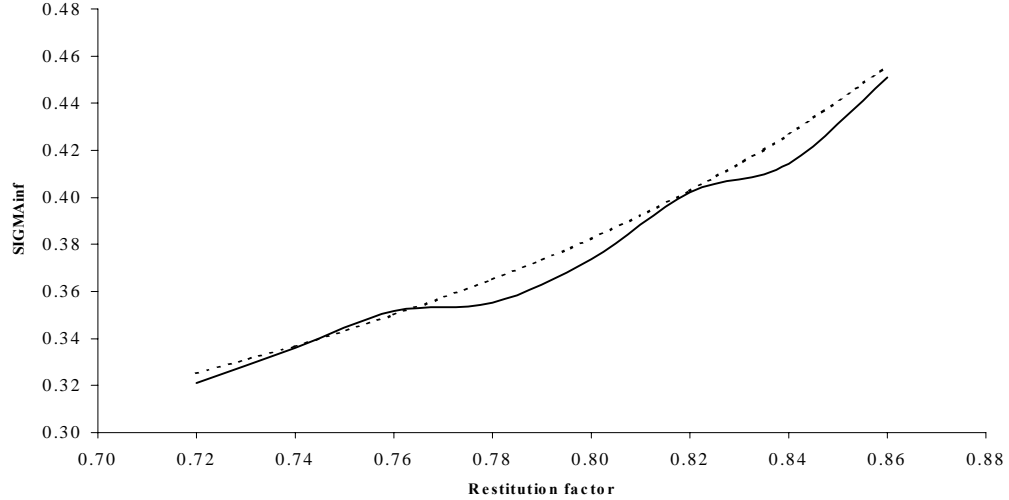


Figure 13. Application of α_{eq} for problem of vibration of secondary structure.

Solid line – numerical result, Dashed line – result of calculation with α_{eq}

Figures 14 represent Monte-Carlo simulation results for $\sigma_z/\sigma_{z\infty}$ vs. Ω_s/Ω are compared with the curves, which are reproduced from (Dimentberg et al., 1998) and are based on analytical solution for autocorrelation function $K_{yy}(\tau)$ for $\alpha/\Omega=0.01$. Good correlation is seen once again between simulation results and the analytical ones, based on the equivalent viscous damping (3.14). The latter is seen therefore as providing a viable simplified approach for incorporating impact losses into random vibration analyses.

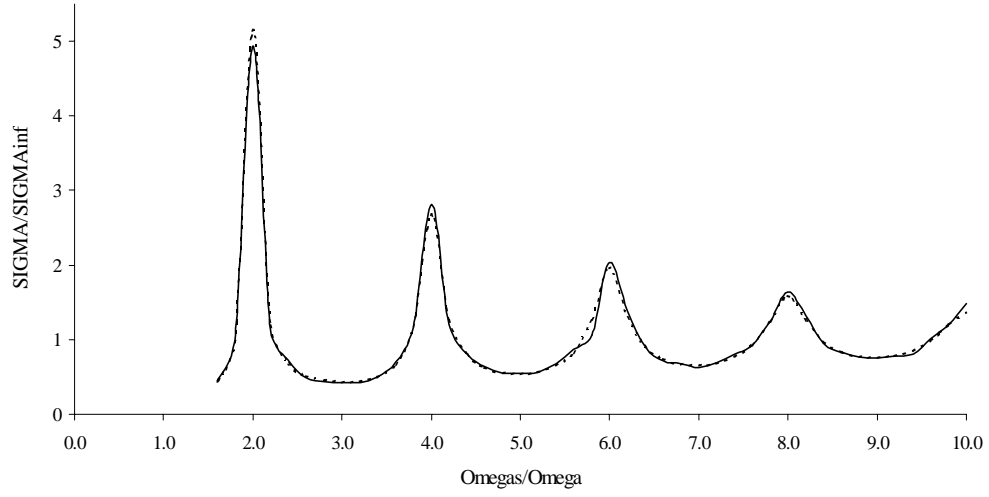


Figure 14. Comparison of analytical with α_{eq} and numerical results.

Solid line – numerical result, Dashed line – result of calculation with α_{eq}

3.4 Piecewise Conservative systems – inertia controlled system

In this section an externally excited SDOF systems is considered that is controlled through system's inertia

$$\frac{d}{dt} \left(J_0 \left[1 + R \operatorname{sgn}(\theta \dot{\theta}) \right] \dot{\theta} \right) + k\theta = \varsigma(t), 0 \leq R < 1 \quad (3.21)$$

This equation may be rewritten, by introducing a new state variable p (Iourtchenko et al., 2000), as two first order SDEs, which are then supplemented with that for the response energy (per unit J_0)

$$\begin{aligned}\dot{\theta} &= \frac{p}{[1 + R \operatorname{sgn}(\theta p)]}, \quad \dot{p} = -\Omega^2 \theta + \bar{\zeta}(t), \quad \text{where } \Omega^2 = k/J_0 \\ E &= \frac{p^2}{2[1 + R \operatorname{sgn}(\theta p)]} + \frac{\Omega^2 \theta^2}{2}, \quad \dot{E} = \frac{p \bar{\zeta}(t)}{[1 + R \operatorname{sgn}(\theta p)]}; \quad \bar{\zeta}(t) = J_0^{-1} \zeta(t)\end{aligned}\tag{3.22}$$

The last Stratonovich SDE is transformed to the Ito one, by applying Wong-Zakai correction, and the conditional averaging is applied then, with condition being initial values of the state variables at $t = 0$. This results in the deterministic equation for the conditional expected energy, which describes linear growth of the response energy between stepwise parameter variations (the notation D is used here for the intensity of the scaled white noise $\bar{\zeta}(t)$, so that the original white-noise excitation in the RHS of the equation (3.21) has intensity DJ_0^2)

$$\dot{\bar{E}} = \frac{D}{2[1 + R \operatorname{sgn}(\theta p)]}, \quad \bar{E} = \bar{E}(0) + \frac{Dt}{2[1 + R \operatorname{sgn}(\theta p)]}\tag{3.23}$$

Consider now variation of the response energy within a half-cycle, which starts slightly to right of the system's equilibrium position (after the stepwise drop of the kinetic energy), so that both state variables are positive at $t = 0$. The random durations of the half-cycle and quarter-cycles are denoted by Θ with subscripts $\frac{1}{2}$ and $\frac{1}{4}$ respectively

and additional “plus” and “minus” subscripts for the quarter-cycles corresponding to the signs in front of R . The system’s energy growth within each quarter-cycle can be obtained, by applying equation (3.23), as

$$\bar{E}(\Theta_{1/4} - 0) = \bar{E}(0) + \frac{D\Theta_{1/4+}}{2[1+R]} \text{ and } \bar{E}(\Theta_{1/2} - 0) = \bar{E}(\Theta_{1/4} + 0) + \frac{D\Theta_{1/4-}}{2[1-R]} \quad (3.24)$$

The total energy does not experience any changes at the system’s extreme positions, whereas total energies before and after stepwise parameter variation at the equilibrium position are related by the continuity condition for the angular momentum p as

$$\bar{E}(\Theta_{1/2} + 0) = \bar{E}(\Theta_{1/2} - 0) \left(\frac{1-R}{1+R} \right) \quad (3.25)$$

Combining equations (3.23), (3.24) and (3.25), one can relate response energy at the end of the half-cycle to that at the start of the half-cycle as

$$\bar{E}(\Theta_{1/2} + 0) = \bar{E}(\Theta_{1/2} - 0) \left(\frac{1-R}{1+R} \right) = \left\{ \bar{E}(0) + \frac{D\Theta_{1/4+}}{2[1+R]} + \frac{D\Theta_{1/4-}}{2[1-R]} \right\} \left(\frac{1-R}{1+R} \right) \quad (3.26)$$

Whilst the response energy varies (randomly) from cycle to cycle, the basic response pattern repeats itself within all half-cycles, and the unconditional averaging (once again denoted by angular brackets) may be applied to equation (3.26). As long as steady-state

response $E(t)$ is a stationary process, its expected value at the instants of zero-crossings by $\theta(t)$, i.e. at $t=0, t=T_{1/2}$, etc. should be a constant, so that

$$\langle \bar{E}(\Theta_{1/2} + 0) \rangle = \langle \bar{E}(0) \rangle = \frac{(D/4\alpha_{eq})}{2}(1-R) \left[\frac{1}{\sqrt{1+R}} + \frac{1}{\sqrt{1-R}} \right],$$

as long as $\langle \Theta_{1/4\pm} \rangle = T_{1/4\pm} = \frac{\pi}{2\Omega} \sqrt{1 \pm R}$

where $\alpha_{eq} = R\Omega/\pi$. The expected time between stepwise parameter variations is once again approximated here by the corresponding natural quarter-periods of the free system (3.21) (without white-noise)

The overall mean energy may be calculated now as the average-over-the-half-period (see (3.12)) of the piecewise-linear conditionally expected energy (3.24)

$$\langle E(t) \rangle = \frac{1}{T_{1/2}} \int_0^{T_{1/2}} \bar{E}(t) dt = \sigma^2 \phi(R); \quad \sigma^2 = D/4\alpha_{eq}, \quad \phi(R) = (1/2)(\sqrt{1+R} + \sqrt{1-R}) \quad (3.27)$$

The first co-factor in the final expression for the expected response energy is clearly seen to correspond to the limiting case $R \ll 1, \phi(R) \cong 1$. This case can be handled by the asymptotic stochastic averaging method. The latter shows also that the system behaves as one with a linear viscous damping, with the “equivalent” damping ratio $\Omega R/\pi$, and the angular response is asymptotically Gaussian, so that the response energy has asymptotically exponential stationary probability density. With increasing R the expected response energy is seen to decrease from its limiting asymptotic value.

These analytical results are compared in Figure 15 with Monte-Carlo simulation data, as shown by the dotted line. The dashed line represents scaled expected response energy

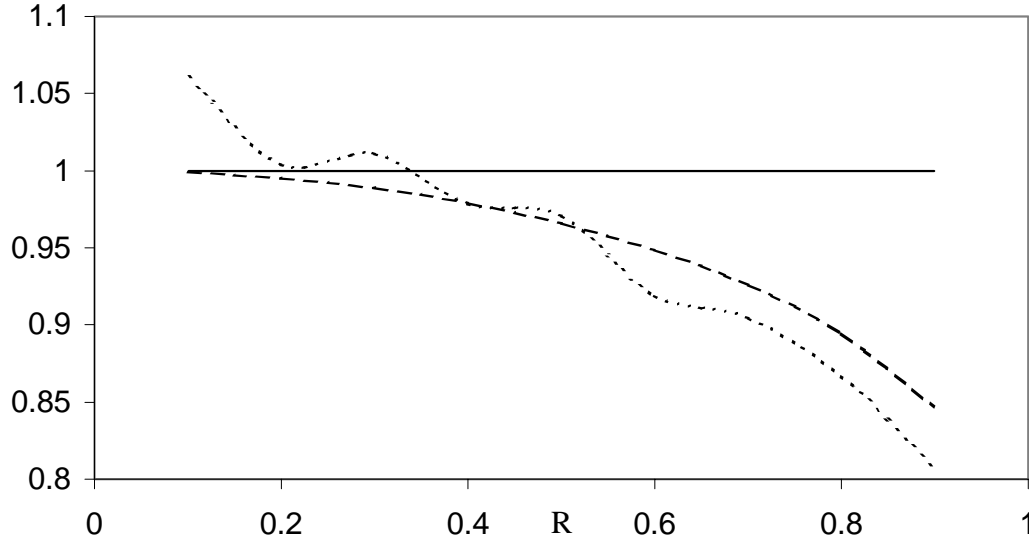


Figure 15. Comparison of results for inertia controlled system.

$\langle E \rangle / \sigma^2$, as calculated according to the formula (3.27), whereas the horizontal solid line is its limiting (unity) value, as obtained by the asymptotic approach. The latter is seen to provide reasonable accuracy (within 5 per cent) up to $R = 0.5$, that is far beyond the expected applicability range of the theory for the supposedly small parameter R . However, the direct energy balance is seen to provide even better results for not-too-small values of R , up to as high as $R = 0.9$.

3.5 Piecewise Conservative systems – stiffness controlled system

Consider the following Piecewise Conservative system subjected to Gaussian white-noise excitation (Iourtchenko et. al. 2000)

$$\frac{d}{dt}(J_0\dot{\theta}) + k[1 + R \operatorname{sgn}(\theta\dot{\theta})]\theta = \zeta(t), 0 \leq R < 1 \quad (3.28)$$

Because the system is piecewise conservative, the energy balance method may be applied to obtain a mean system's response energy.

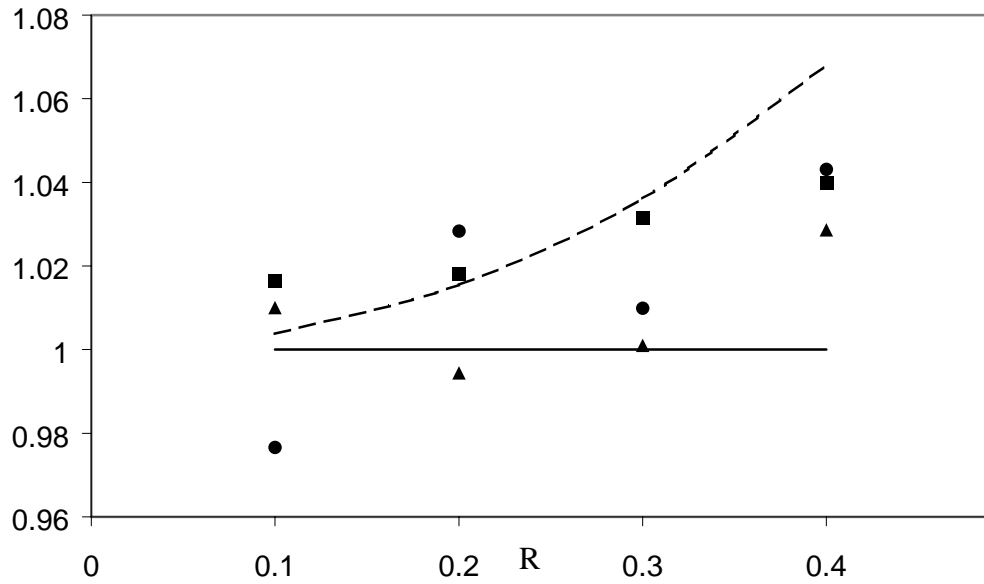


Figure 16. Comparison of results for stiffness controlled system.

The direct energy balance approach (dashed line) and Monte-Carlo simulation for the following values of the excitation intensity: circle -- $D = 10$, triangle -- $D = 1$, square -- $D = 0.5$

0.1. The horizontal line represents the asymptotic (stochastic averaging) value for small R .

Following the procedure, established in previous sections, one may obtain the following expression for a mean energy (Iourtchenko 2000)

$$\langle E \rangle = \sigma^2 \psi(R), \quad \psi(R) = (1/2) \left[(1+R)^{-1/2} + (1-R)^{-1/2} \right] \quad (3.29)$$

with the same expressions for σ and α_{eq} as before.

These analytical results for $\langle E \rangle / \sigma^2$ are represented in Figure 16 by the dashed line, whereas the horizontal solid line represents the limiting (unity) asymptotic value. Comparison with Monte-Carlo simulation data, shown by various symbols for three different values of D (and $\Omega = 1$) indicates reasonable accuracy of both analytical approaches within the range $R < 0.4$ – once again, even for not-very-small R 's.

3.6 Piecewise Conservative systems – pendulum with variable length

In this Section, problem of pendulum with variable length will be discussed briefly. Consider the following dynamic system (Dimentberg 2000), equation of motion of which may be written as

$$\begin{aligned} (d/dt)(L^2 \dot{\theta}) + gL\theta &= -L\zeta(t) \\ L &= L_0 [1 + R \operatorname{sgn}(\theta \dot{\theta})] \end{aligned} \quad (3.30)$$

Similar to the problem with inertia control, a new variable p may be introduced here for convenience. Then, applying the Energy Balance method, the following expression for a mean system's response energy may be derived

$$\begin{aligned}
\langle E \rangle / gL_0 &= \sigma^2 \phi_L(R), \\
\phi_L(R) &= \phi_0(R) - \frac{3}{2} R (\sqrt{1+R} + \sqrt{1-R}) - \frac{4R [\phi_0(R) + 3R\sqrt{1-R}]}{(1+R)^{3/2} (\sqrt{1+R} + \sqrt{1-R})} \\
\sigma^2 &= D_\xi \Omega^2 / 4\alpha_{eq}, \quad D_\xi = D / g^2, \quad \alpha_{eq} = 3\Omega R / \pi \\
\phi_0(R) &= (1/2)(1-R) \frac{[(1+R)^{5/2} + (1-R)^{5/2}]}{(1+R^2/3)}
\end{aligned} \tag{3.31}$$

where D_ξ is seen to be the intensity of the non-dimensional horizontal support acceleration in g's. Once again, in the asymptotic case of small R the system behaves as one with the linear damping; the equivalent damping ratio, however, is found to be three times higher than for the system with inertia and stiffness control. This case is represented in Figure 17 by a solid horizontal line at the unit height, where scaled expected response energy $\langle E \rangle / gL_0 \sigma^2$ is given as a function of R .

The dashed line represents results of the Monte-Carlo simulations, whereas the dotted line represents the analytical solution (3.31). The latter is seen to provide some improvement of accuracy compared with the asymptotic (stochastic averaging) approach.

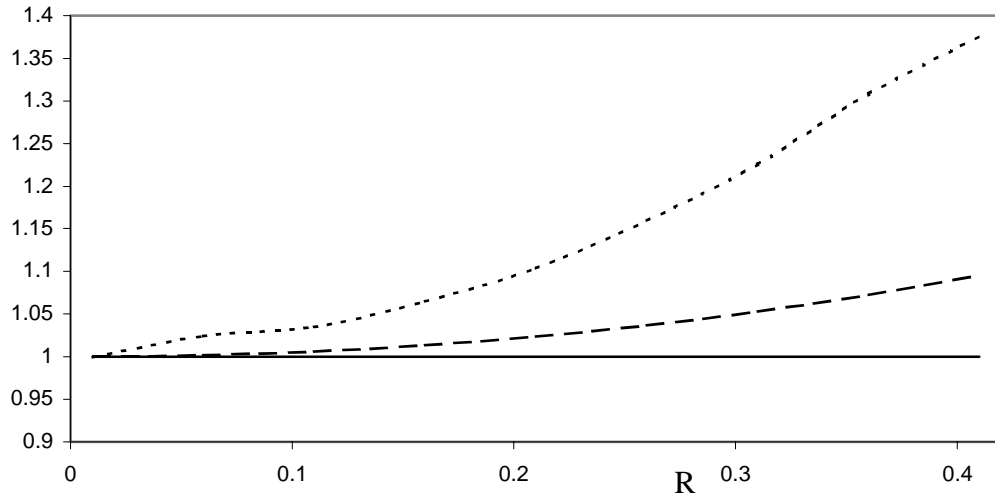


Figure 17. Comparison of results for a pendulum with variable length (swings).

Scaled expected response energy $\langle H \rangle / gL_0\sigma^2$ vs. R according to the analytical solution by the direct energy balance approach - dashed line, Monte-Carlo simulation - dotted line and stochastic averaging method valid value for small R – solid line

3.7 The Energy Balance method for a SDOF system with dry friction

Consider now a SDOF system with Coulomb, or dry friction damping, as governed by the following equation of motion (Dimentberg et al., 1999)

$$\ddot{x} + R \operatorname{sgn} \dot{x} + \Omega^2 x = \zeta(t), \quad \text{where } R > 0$$

$$\operatorname{sgn} \dot{x} = +1 \text{ for } \dot{x} > 0, \operatorname{sgn} \dot{x} = -1 \text{ for } \dot{x} < 0$$
(3.32)

This equation may also appear for a system with active response control, whenever magnitude of the control force is bounded, as long as the dry-friction control law is found to be the optimal one to reduce the steady-state expected response energy $\langle E \rangle$. Namely, replacing the second term in the LHS of the equation (3.32) by any other control law $u(x, \dot{x}, t)$ with $|u| \leq R$ may only increase $\langle E \rangle$.

Introducing the response energy E , the equation of motion (3.32) may be rewritten in a space-state form as

$$\begin{aligned} \dot{x}_1 &= x_2, \dot{x}_2 = -\Omega^2 x_1 - R \operatorname{sgn} x_2 + \zeta(t), \\ E &= (1/2)(\Omega^2 x_1^2 + x_2^2), \langle \dot{E} \rangle = -R|x_2| + x_2 \zeta(t) \end{aligned} \quad (3.33)$$

A conditional averaging is applied to this set of “physical” or Stratonovich stochastic equations (SDEs) (Dimentberg 1988, Lin et al., 1995) denoted by bar, with condition being given values of state variables at a certain selected time instant. Using Wong-Zakai correction for $E(t)$ yields

$$\bar{\dot{E}} = -R|x_2| + D/2 \quad (3.34)$$

The ODE (3.34) may be integrated directly within any time interval that does not contain reversals of velocity. The resulting variation of the conditional mean energy will be $R s + D t / 2$, where s is the traversed distance. Let this distance will be just the instantaneous range $x_{peak} - x_{trough}$, denoted as $2A$, or doubled response amplitude, where the

initial and final instant of time correspond to the pair of consecutive trough and peak of $x(t)$. Then the unconditional averaging for steady-state response results in

$$\langle \Delta \bar{E} \rangle = -2R \langle A \rangle + DT/2 \cong -2R \langle A \rangle + D\pi/2\Omega = 0, \text{ so that } \langle A \rangle \cong D\pi/4\Omega R \quad (3.35)$$

Here T is the expected value of the time interval between the consecutive trough and peak, which once again is approximated here by the system's natural half-period. The resulting expression for the expected response amplitude is found to be the same as obtained by stochastic averaging. However its range of applicability should not be restricted by the condition for small D and R , as long as the energy balance approach does not require the variations of energy to be small within any response cycle.

Table 2 presents numerical (Monte-Carlo) simulation data for the expected response amplitude, normalized with respect to the “dead zone” $\Delta = R/\Omega^2$. These data are compared with calculations according to the energy-balance formula (3.35), which yields $\langle A \rangle / \Delta = \pi/4\mu^2$, where $\mu = R/\sqrt{D\Omega}$ is a nondimensional parameter of the “dry-friction” force. The agreement is seen to be very good for values of μ , small compared with unity. It is also reasonably good for values of the order of unity – that is, far beyond the expected range of applicability of the asymptotic methods. (In actual numerical simulations values $D = 1$ and $\Omega = 1$ were assigned, whereas R was varied).

	$\mu=1.414$	$\mu=1.0$	$\mu=0.8$	$\mu=0.5$	$\mu=0.2$
Analytical	0.3927	0.7854	1.2272	3.1416	19.635
Numerical	0.3353	0.7118	1.141	3.0788	19.58

Table 2. Nondimensional expected response amplitudes $\langle A \rangle \Omega^2 / R$ vs. $\mu = R/\sqrt{D\Omega}$.

3.8 Reliability analysis of a SDOF system with dry friction

Whilst formula (3.35) provides some estimates of the stationary response level for the optimally controlled system, more sophisticated response characteristics may be of interest for predicting reliability of the system. Their analysis is rather straightforward for the limiting case of a weak control. Indeed, if both R and D are proportional to a small parameter, the original SDE can be reduced efficiently by applying stochastic averaging method. Both “regular” and quasiconservative versions of the method can be used for the quasilinear system

According to the quasiconservative averaging method [11, 28], the velocity state variable in the RHS of the SDE (3.33) for E is expressed as $x_2 = v = \sqrt{2E - \Omega^2 x_1^2}$. This RHS is averaged then over “rapid” time within response period $2\pi/\Omega$, with slowly varying energy E being kept constant; in view of symmetry, a quarter of period can be considered only. The integration according to this averaging can be replaced by that over “fast” state variable x from zero to A , as long as $dx = v dt$. Here $A = \sqrt{2E}/\Omega$ is amplitude, or maximal displacement within a response cycle with given energy E . Applying the procedure to both terms in the RHS of the SDE (3.33) for E and adding Wong-Zakai correction $D/2$, yields the following approximate first-order Ito SDE for the response energy

$$\dot{E} = -\left(2R\sqrt{2}/\pi\right)\sqrt{E} + D/2 + \sqrt{DE}\zeta(t) \quad (3.36)$$

From this equation formula (3.35) for the mean response amplitude can be obtained immediately, by imposing condition for zero expectation of the RHS and using the relation between A and E . Furthermore, the Fokker-Planck-Kolmogorov (FPK) equation can be written for $p(E)$ - probability density function (p.d.f.) of E - which corresponds to the SDE (3.36). This equation has the following stationary solution

$$p(E) = (\gamma^2/2) \exp(-\gamma\sqrt{E}), \gamma = 8R\sqrt{2}/\pi D, \text{ so that } \langle E \rangle = 6/\gamma^2 = (3\pi^2/64)(D/R)^2 \quad (3.37)$$

Consider a vibrating component with possibility for a first-passage failure after exceeding a certain given response energy threshold E_* . Assuming the initial energy E to be smaller than this threshold, we may consider an expected time T for reaching it, as long as the system's dynamics is described approximately by the first-order SDE (13). The function $T(E)$ in this case satisfies the following deterministic ODE, its coefficients being derived from those of the SDE (3.36) as described in [11]

$$(DE/2)(d^2T/dE^2) + [D/2 - (2R\sqrt{2}/\pi)\sqrt{E}](dT/dE) = -1 \quad (3.38)$$

The boundary conditions for this equation are (see an extensive discussion of the first one in [28])

$$dT/dE = -2/D \text{ at } E = 0; T(E_*) = 0 \quad (3.39)$$

The first integration of the equation (3.38) yields, after imposing the first BC (3.39) (at $E = 0$)

$$dT/dz = \frac{(1 + 2\lambda\sqrt{z} - \exp 2\lambda\sqrt{z})}{(4\lambda^2\Omega z)}, \quad z = E/(D/4\Omega), \lambda = 2\mu\sqrt{2}/\pi, \mu = R/\sqrt{D\Omega} \quad (3.40)$$

Whilst this expression is convenient for numerical integration, it has the analytical solution, which satisfies the second BC (3.39)

$$T(z) = [Ei(2\lambda\sqrt{z_*}) - Ei(2\lambda\sqrt{z})]/2\Omega\lambda^2 - (\sqrt{z_*} - \sqrt{z})/\Omega\lambda - (4\Omega\lambda^2)^{-1} \ln(z_*/z) \quad (3.41)$$

Here Ei is an exponential integral function

$$Ei(x) = - \int_{-x}^{\infty} \frac{e^{-t}}{t} dt$$

Consider now the case of a fatigue-type failure. According to a simple model of linear fatigue damage accumulation, the expected fatigue life is inversely proportional to the m -th-order moment of the stress amplitude [11], and thus to the moment of response energy of the order $m/2$; here m is a parameter of stress-life curve for the material (its slope in semi-log coordinates). For a structure with linear viscous damping the model leads to a well-known Miles' formula [11], which can be used for comparison of two different types of damping on the basis of the same expected response energy. For the optimally controlled system - one with the dry-friction damping - the corresponding moment of the probability density $p(E)$ (3.37) may be calculated for even integer m as

$\langle E^{m/2} \rangle_{DRY} = (m+1)!/\gamma^m$. On the other hand, probability density of energy in the system with linear damping is $p(E) = \sigma_v^{-2} \exp(-E/\sigma_v^2)$, where σ_v^2 is a mean square response velocity and $\langle E^{m/2} \rangle_{VISC} = \sigma_v^m (m/2)!$ for even integer m . Thus, equating two expressions for $(m/2)$ -th-order moments of E for $m = 2$, yields the condition for comparable response levels as $\sigma_v \gamma = \sqrt{6}$. The expected life ratio for the two types of damping is then found to be $T_{DRY}/T_{VISC} = [6^{m/2} (m/2)!]/(m+1)!$

The last formula clearly shows the system with dry-friction damping - which is the best kind of damping that can be obtained by using optimal bounded control - to be less reliable than the system with linear damping and same mean square response level. If the linear damping is produced by velocity feedback control, this reduction of reliability may be interpreted as a price for the imposed bound on control force, or for “weak” actuators. The price is seen to increase with m , i.e. it is higher for materials which are more sensitive to stress cycles with higher amplitudes; thus, the above ratio equals just 0.6 for $m = 4$, is reduced to about 0.25 for $m = 6$ and then becomes much less than 0.1 for $m = 8$.

3.9 Conclusions

A certain class of nonlinear random vibration problems has been considered for Piecewise Conservative systems under white-noise excitation. The direct Energy Balance has proved itself to be an efficient and accurate approach for predicting (nonlinear) response of “piecewise-conservative” systems to white-noise random excitations for

those cases, where simple estimate of the expected response level (expected energy) is sufficient for the given application. In particular, the method may be convenient for estimating efficiency of the active feedback control systems, based on the use of “bang-bang” control laws. Such estimates may be used as important benchmarks, in spite of the fact that in real-life applications a low-pass filter may be included into the feedback loop in order to avoid high-frequency chatter, whereas excitation may be not a white noise but rather just a broadband random process. Monte-Carlo simulation studies for a variety of specific problems indicate reasonable accuracy of the method far beyond the expected applicability range of the asymptotic approaches, especially for vibroimpact systems – for values of a supposedly small (compared with unity) nondimensional parameter up to 0.4 and higher. However, the accuracy of the method is much better for the case of inertia and stiffness controlled system than for one with controlled length.

4. Main Findings

In this section the important results and conclusions of the above work will be summarized briefly.

- An exact analytical solutions to the Hamilton-Jacobi-Bellman equation has been obtained within the “outer” domain” for the Mayer, Lagrange and Boltz cost functions.
- These solutions are exact and therefore are valid for any, not necessary small values of R and σ
- An exact analytical solution indicated that the dry-friction control law is a suboptimal control law for Mayer cost function.
- It has been proved that for a steady-state system’s response, the dry-friction control law is an optimal one for a mean system’s response energy reduction.
- A direct numerical simulation of the Hamilton-Jacobi-Bellman equation has been performed using the above analytical solutions as boundary conditions for the corresponding cost function.
- Extension to the case of multi-degree-of-freedom system has been derived for the Mayer and Lagrange cost functions.
- Reliability analysis for “optimally controlled” single-degree-of-freedom system has shown that this system is less reliable than the one with viscous damping.

- A new Direct Energy Balance method has been developed and implemented for various types of piecewise conservative systems.
- Comparison with the stochastic averaging method and direct Monte Carlo simulation demonstrated that the Energy Balance method provides better accuracy than stochastic averaging one and may be applied far beyond the applicability range of the latter.

5. Recommendations and future work

The Hybrid Solution method, proposed and developed in the foregoing Sections proved to be very effective for solution of stochastic optimal control problems via Dynamic Programming approach. The possibility of obtaining an exact analytical solution greatly simplify problem of finding an optimal control law. Moreover, certain important conclusions may be derived directly from an analytical solution, as it has been shown in the case of Lagrange cost function.

Solution to the vibroimpact problem has been obtained using the hybrid solution method (Bratus et al., 2000). Application of the method may be extended to different systems and different types of excitations, acting onto the system. One of them is a linear system subjected to Poisson noise. The difference-differential HJB equation will appear and has to be solved. The other important application is identifying an optimal control law for parametrically (stiffness) controlled systems. The control law in this case will lead to the equation of motion, similar to one (3.28) considered in Section 3.5. This optimal control law may find its application in modeling smart material. Finding an optimal control for a system subjected to random and harmonic excitation is also possible by means of the hybrid solution method.

Although the Energy Balance method is possible to apply only to piecewise conservative systems, certain helpful information may be obtained using this method, besides an expression for mean system's response energy. Namely, finding an exact solution to the First Passage problem is extremely mathematically and numerically complex problem. However, using an exact analytical expression for mean energy in

terms of mean cycle duration time T , one can easily obtain the latter, based on simple measurements of mean system's energy through Monte Carlo simulation of equation of motion. This approach obviously is much easy than numerical simulation of First Passage problem, which is represented as a multidimensional partial differential equation.

References

1. Anderson D., Townehill J. and Pletcher R., Computational Fluid Mechanics and Heat Transfer, v. 1, Hemisphere, New York, 1984
2. Bensoussan A., Perturbation Methods in Optimal Control. John Wiley, New York, 1988.
3. Bensoussan A., Stochastic Control of Partially Observable Systems, Cambridge Universal Press, 1992.
4. Boyd S.P. and Barratt C.H.. Linear Controller Design: Limits of Performance. Prentice Hall, Edgewood Cliffs, 1991.
5. Bratus A.S., "Numerical solutions for the problems of control in a random media" (in Russian). Space Research 9 (4), 1971.
6. Bratus A.S., "Approximate solution of the HJB equation for a system under a random excitation", Journal of Applied Mathematics and Mechanics, v 39, 1975.
7. Bratus A.S., "Asymptotic Solution for Certain Problems of Optimal Control with Probability", (In Russian), Journal of Applied Mathematics and Mechanics, v.41, 1977.
8. Bratus A., Dimentberg M.F. and Iourtchenko D.V., "Optimal bounded response control for a second-order system under a white-noise excitation". Journal of Vibration and Control, v 6, No 5, pp. 741-755, 2000.
9. Bratus A., Dimentberg M.F., Iourtchenko D.V. and Noori M.N., "Hybrid solution method for dynamic programming equations for MDOF stochastic systems". Dynamics and Control, v 10, No 1, pp. 107-116, 2000.

10. Chernousko F.L. and Kolmanovskii V.B.. Optimal control for systems under random excitations. (in Russian) Nauka, Moscow, 1978.
11. Dimentberg M.F. Statistical Dynamics of Nonlinear and Time-Varying Systems. Research Studies Press, Taunton, UK, 1988.
12. Dimentberg M.F and Haenisch H. G., “Pseudolinear Vibroimpact System with a Secondary Structure: Response to a White-Noise Excitation”. Journal of Applied Mechanics, vol. 65, No 3., pp 772, 1998
13. Dimentberg M.F., Iourtchenko D.V. & Otto van Ewijk. “Subharmonic response of a quasiisochronous vibroimpact system to a randomly disordered periodic excitation”. Nonlinear Dynamics, v 17. No 2, 1998.
14. Dimentberg M.F., Haenisch H. G. & Iourtchenko D.V. “Response of a vibroimpact system with secondary structure to a white-noise excitation: case of inelastic impacts”. Proceedings of the ISIFSS 98, Series B, v 14, World Scientific Publishing Co., 2000.
15. Dimentberg M.F. and Iourtchenko D.V. “Towards Incorporating Impact Losses into Random Vibration Analyses: a Model Problem”. Probabilistic Engineering Mechanics, vol. 14, 1999, pp.323 – 328.
16. Dimentberg M.F., Iourtchenko D.V. and Bratus A., “Optimal bounded control of steady-state random vibrations”. Probabilistic Engineering Mechanics, v 15, No 4, pp. 381-386, 2000.
17. Dimentberg M.F. and Bratus A., “Bounded Parametric Control of Random Vibrations”. Proceedings of the Royal Society, ser. A, 456, pp.1-13, 2000.

18. Dimentberg M.F. "On a Theory of Swings". Submitted to the Proceedings of the Royal Society, ser. A, 2000.
19. Dreyfus S.E., Dynamic programming and the calculus of variations. Academic Press, New York and London, 1965.
20. Fleming W.H and Rishel R., Deterministic and Stochastic Optimal Control. Springer-Verlag, Berlin, 1975.
21. Friedman A, Stochastic Differential Equations and Applications, Academic Press, New York, 1975
22. Gikhman I. and Skorohod A, Stochastic Differential Equations, Berlin, New York, Springer-Verlag, 1972.
23. Iourtchenko D.V., "Stochastic optimal bounded control for a system with the Boltz cost function". Journal of Vibration and Control, v 6, No 8, pp. 1195-1204, 2000.
24. Iourtchenko D.V., Dimentberg M.F. and Bratus A., "Optimal control of random vibrations by bounded stiffness variations". 20th International Congress of Theoretical and Applied Mechanics (ICTAM 2000), August 2000, Chicago, IL, USA. Published in ICTAM 2000, International Union of Theoretical and Applied Mechanics, Technical Report No 950.
25. Iourtchenko D.V. and Dimentberg M.F., "Energy balance for random vibrations of piecewise-conservative systems". Accepted to Journal of Sound and Vibration, May 2001.
26. Kolmanovskii V.B. and Shaikhet L.E. Control of systems with aftereffect. American Mathematical Society, Providence, RI, 1996.

27. Kovaleva A.S., Control of Oscillatory and Vibroimpact Systems (in Russian). Publishing House "Nauka", Moscow, 1990.
28. Lin Y.K. & Cai G.Q. Probabilistic Structural Dynamics. McGraw Hill, New York, 1995.
29. Meirovitch L., Elements of Vibration Analysis, McGraw-Hill Book Co., 1986.
30. Stengel R.F., 1986, Stochastic Optimal Control, Theory and Application, John Wiley & Sons, USA.
31. Zhu W.Q., Ying Z.G. and Sonong T.T., "Optimal nonlinear feedback control of structures under random loading", 4th International Conference on Stochastic Structural Dynamics, August 1998, Notre Dame, IN, USA. Published in Stochastic Structural Dynamics, A.A. Balkema Publisher 1999, Rotterdam, Netherlands.
32. Zhuravlev V.F. A Method for analyzing vibration-impact systems by means of special functions. Mechanics of Solids, 11, 1976, pp. 23 - 27 (English translation of the Russian Journal Mekhanika Tverdogo Tela).
33. Zhuravlev V.F. and Klimov D.M. Applied Methods in Vibration Theory (in Russian). Moscow, Nauka, 1988.
34. Yoneyama T., "Adjoint processes in stochastic optimal control problems". International Journal of Control, 39 (3), 423 – 431, 1984.